



# Kent Academic Repository

**Dora, Nova Olympia (2020) *Development of novel antimicrobials as potential anticancer treatments*. Master of Science by Research (MScRes) thesis, University of Kent,.**

## Downloaded from

<https://kar.kent.ac.uk/81198/> The University of Kent's Academic Repository KAR

## The version of record is available from

## This document version

UNSPECIFIED

## DOI for this version

## Licence for this version

UNSPECIFIED

## Additional information

## Versions of research works

### Versions of Record

If this version is the version of record, it is the same as the published version available on the publisher's web site. Cite as the published version.

### Author Accepted Manuscripts

If this document is identified as the Author Accepted Manuscript it is the version after peer review but before type setting, copy editing or publisher branding. Cite as Surname, Initial. (Year) 'Title of article'. To be published in **Title of Journal**, Volume and issue numbers [peer-reviewed accepted version]. Available at: DOI or URL (Accessed: date).

### Enquiries

If you have questions about this document contact [ResearchSupport@kent.ac.uk](mailto:ResearchSupport@kent.ac.uk). Please include the URL of the record in KAR. If you believe that your, or a third party's rights have been compromised through this document please see our [Take Down policy](https://www.kent.ac.uk/guides/kar-the-kent-academic-repository#policies) (available from <https://www.kent.ac.uk/guides/kar-the-kent-academic-repository#policies>).



# **Development of novel antimicrobials as potential new anticancer treatments**

**Nova Olympia Dora**

Thesis for MSc by Research in Cell Biology

School of Biosciences

University of Kent

Supervisors:

Professor Michelle Garrett

Dr Jennifer Hiscock

## **Declaration**

No part of this thesis has been submitted in support of an application for any degree or qualification of the University of Kent or any other university or institute of learning.

Nova Olympia Dora

## **Acknowledgements**

I would like to thank my supervisors Professor Michelle Garrett and Dr Jennifer Hiscock for their support and guidance with this project.

Special thanks go to Edith Blackburn for all her help and support in the lab throughout this year.

I would also like to thank Dan, Nathan, Jasmine, Helen, Eithaar, Timo and Natasha for making the lab an enjoyable environment to work in and helping along the way.

I would like to thank some members of the Hiscock group; Lisa, Nya and Jess for their help with the chemistry side of this project. I would also like to thank Professor Dan Mulvihill for helping me carry out microscopy experiments.

Lastly I would like to thank my family for their ongoing support throughout my last 4 years at university.

## Contents

<b>Declaration</b> .....	<b>2</b>
<b>Acknowledgements</b> .....	<b>3</b>
<b>Abbreviations</b> .....	<b>6</b>
<b>List of figures</b> .....	<b>8</b>
<b>Abstract</b> .....	<b>9</b>
<b>1. Introduction</b> .....	<b>10</b>
<b>1.1 Cancer</b> .....	<b>10</b>
<b>1.2 Ovarian cancer</b> .....	<b>10</b>
1.2.1 Ovarian cancer treatment.....	11
<b>1.3 Brain cancer</b> .....	<b>12</b>
1.3.1 Brain cancer: Symptoms .....	14
1.3.2 Brain cancer: Diagnosis.....	15
1.3.3 Brain cancer: Treatments .....	15
<b>1.4 Chemotherapy</b> .....	<b>17</b>
<b>1.5 Novel antimicrobial compounds</b> .....	<b>18</b>
1.5.1 Compound structure.....	22
<b>1.6 Composition of cancer cells compared to normal cells</b> .....	<b>23</b>
<b>1.7 Membrane lipid composition</b> .....	<b>23</b>
<b>1.8 Differential membrane composition of brain tumour cells</b> .....	<b>24</b>
<b>1.9 Project aims</b> .....	<b>25</b>
<b>2. Materials and Methods</b> .....	<b>27</b>
<b>2.1 Cell Lines</b> .....	<b>27</b>
<b>2.2 Compounds</b> .....	<b>27</b>
<b>2.3 Cell culture</b> .....	<b>27</b>
<b>2.4 Cell Seeding Density assays</b> .....	<b>28</b>
<b>2.5 SRB assays</b> .....	<b>28</b>
<b>2.6 Combination studies</b> .....	<b>29</b>
2.6.1 Chou-Talalay assay.....	29
2.6.2 Combination assay.....	29
<b>2.6 Immunofluorescence</b> .....	<b>30</b>
<b>2.7 Western Blot analysis</b> .....	<b>30</b>
<b>3. Results</b> .....	<b>34</b>
<b>3.1 Cell lines</b> .....	<b>34</b>
<b>3.2 Cell density seeding assay</b> .....	<b>35</b>
3.2.2 A2780 Seeding Density .....	36
3.2.3 U87MG Seeding Density .....	37
<b>3.3 Toxicity assay and IC<sub>50</sub> determination</b> .....	<b>38</b>
3.3.1 Toxicity graphs of each compound on A2780 cells .....	40
3.3.2 Toxicity graphs of each compound on U87MG cells .....	41
<b>3.4 Combination studies</b> .....	<b>42</b>
3.4.1 Chou-Talalay assay.....	42

3.4.2 Drug combination assay.....	45
<b>3.5 Western blot analysis .....</b>	<b>47</b>
3.5.1 Cleaved PARP .....	49
3.5.2 Cell signalling targets .....	49
3.5.3 Cell cycle proteins .....	50
3.5.4 Western blot of Gamma H2AX .....	52
<b>3.6 Immunofluorescence .....</b>	<b>53</b>
<b>4. Discussion .....</b>	<b>56</b>
<b>4.1 Intro.....</b>	<b>56</b>
<b>4.2 SRB analysis .....</b>	<b>56</b>
<b>4.3 Chou Talalay.....</b>	<b>57</b>
<b>4.4 Combination studies.....</b>	<b>58</b>
<b>4.5 Western .....</b>	<b>59</b>
4.5.1 DNA damage .....	59
4.5.2 Cell signalling targets .....	61
4.5.3 Cell cycle proteins .....	62
<b>4.6 Immunofluorescence .....</b>	<b>63</b>
4.6.1 Tumor visualizing agent .....	65
<b>4.7 Future works .....</b>	<b>66</b>
4.7.1 Further combination studies .....	66
4.7.2 Immunofluorescence .....	67
4.7.3 Protein analysis .....	67

## **Abbreviations**

**AKT** – Protein kinase B

**ATR** – Ataxia telangiectasia mutated and Rad3 related kinase

**ATM** – Ataxia telangiectasia mutated kinase

**BSA** – Bovine serum albumin

**CDK** – Cyclin dependent kinase

**Chk1** – Checkpoint kinase 1

**CKI** – Cyclin-dependent kinase inhibitor

**CPW** – Cells per well

**DESI-MS** – Desorption electrospray ionization mass spectrometry

**E. Coli** – Escherichia coli

**ECL** – Enhanced chemiluminescence

**FBS** – Fetal bovine serum

**FDA** – Food and drug administration

**GAPDH** – Glyceraldehyde 3-phosphate dehydrogenase

**GBM** – Glioblastoma multiforme

**HBA** – Hydrogen bond accepting

**HBD** – Hydrogen bond donating

**HRP** – Horseradish peroxidase

**IC** – Inhibitory concentration

**ICR** – Institute of Cancer Research

**IMDM** – Iscove's Modified Dulbecco's Medium

**IDH1** – Isocitrate dehydrogenase 1

**MAPK** – Mitogen activated protein kinase

**MGMT** – O<sup>6</sup>-methylguanine-DNA methyltransferase

**MRSA** – Methicillin resistant staphylococcus aureus

**PARP** – Poly (ADP-ribose) polymerase

**PBS** – Phosphate buffered saline

**PI3K** – Phosphoinositide 3 kinase

**PVDF** – Polyvinylidene difluoride

**SRB** – Sulfurhodamine B

**SSA** – Supramolecular self-associating antimicrobial

**TBST** – Tris buffered saline tween

**TBA** – Tetra butyl ammonium

**TCA** – Trichloroacetic acid

**TMA** – Tetra methyl ammonium

**TPA** – Tetra propyl ammonium

**VEGF** – Vascular endothelial growth factor

**WHO** – World health organization

**$\gamma$ H2AX** – Gamma H2AX

**5-ALA** – 5- Aminolevulinic acid

## List of figures

Figure 1.1: Cisplatin molecular structure

Figure 1.2: Observed and projected age standardized incidence rates of Brain cancer, by sex, UK 1979-2035

Figure 1.3: General structure of novel amphiphilic compounds

Figure 1.4: Molecular structure of fluorescent compound 31, and below a single crystal X-ray structure of this compound in dimer form, through urea-anion complex formation

Figure 1.5: Molecular structures of the series of compounds selected for mammalian testing in this project

Figure 3.1: Microscope images of A2780 cells in culture

Figure 3.2: Microscope images of U87MG cells in culture.

Figure 3.3: Cell seeding density graph on linear scale (A) and logarithmic scale (B) for A2780 ovarian carcinoma cell line.

Figure 3.4: Cell seeding density graph on linear scale (A) and logarithmic scale (B) for U87MG glioblastoma cell line.

Figure 3.5: Cell viability curves of A2780 cells treated with Compound 1, 3, 9, 11, 14, 30, 31 and Cisplatin for 96 hours.

Figure 3.6: Cell viability curves of U87MG cells treated with Compound 1, 3, 9, 11, 14, 30, 31 and Cisplatin for 96 hours.

Figure 3.7: Graph showing effects of Cisplatin and Compound 1 both alone and in combination on A2780 cells.

Figure 3.8: Graph showing effects of Cisplatin and Compound 31 both alone and in combination on A2780 cells.

Figure 3.9: Graph showing effects of Cisplatin alone and with different concentration of Compound 1 on A2780 cells.

Figure 3.10: Western blot of A2780 cells treated with high and low concentrations of Compound 1 and Cisplatin.

Figure 3.11: Western blot of gamma H2AX in A2780 cells treated with high and low concentrations of Compound 1 and Cisplatin.

Figure 3.12: Immunofluorescence of A2780 cells treated with Compound 31 (2-35) for 1 hour.

Figure 3.13: Fluorescence microscopy images of A2780 cells.

Figure 3.14: Fluorescence microscopy images of U87MG cells.

## **Abstract**

One of the first line treatments for most cancers is chemotherapy. Whilst it is generally an effective form of treatment, standard chemotherapy drugs, such as cisplatin, tend to have harmful side effects resulting in a poorer quality of life for patients. A series of novel amphiphilic compounds which were previously shown to be toxic against gram positive and gram negative bacteria were tested to evaluate their potential as an anticancer treatment based on the similarities observed between bacterial cell and cancer cell membranes. To explore the mechanism of action of these compounds, various techniques were used such as SRB analysis, immunofluorescence, western blotting and combination studies. Although these compounds were not deemed to be significantly toxic by themselves, they did appear to show some synergistic effects when combined with cisplatin, a widely used chemotherapeutic agent and the intrinsically fluorescent compounds were shown to bind cancer cell membranes through immunofluorescence. This indicates potential development of these SSA compounds as cancer therapeutics both as a chemotherapy enhancing agent and possibly as a fluorescent biomarker for surgery.

## **1. Introduction**

### **1.1 Cancer**

Cancer remains one of the worlds most critical health issues today. WHO defines cancer as “the uncontrolled growth and spread of cells”<sup>1</sup> caused by mutations in a cells own genetic material. Mutations are more likely to occur due to exposure to certain risk factors, such as tobacco smoke and UV radiation. Once a bodys cells start to abnormally divide, they may also be able to spread to other areas of the body by metastasis; resulting in more complicated, harder to treat cancers.

Although the mortality rate for cancer has decreased by about 16% in the UK since the 1970s, cancer is still one of the leading causes of death. According to Cancer Research UK, there were approximately 18 million new cases of cancer worldwide in 2018, with 9.6 million deaths<sup>2</sup>.

### **1.2 Ovarian cancer**

Ovarian cancer is one of the most common cancers affecting women, with approximately 7,500 new cases diagnosed each year in the UK. It is a disease affecting particularly older women, with more than a quarter (28%) of cases diagnosed in women over the age of 75<sup>2</sup>. Ovarian cancer has a low survival rate as the symptoms do not tend to show until the tumor is more advanced, and has often metastasized. This means the tumor is usually not detected until a later stage, at which point it becomes

more difficult to treat. The first line of treatment is cytoreductive surgery to remove the bulk of the tumor, which is normally followed by chemotherapy.

### 1.2.1 Ovarian cancer treatment

Chemotherapy is an important part of treatment for ovarian cancer, being included in the primary care plan for 54% of patients. The leading form of chemotherapy is platinum based drugs such as Cisplatin (Cis-diamminedichloroplatinum (II)). Cisplatin is an alkylating agent which causes intrastrand adducts on DNA resulting in initiation of the DNA repair pathway. **Figure 1.1** shows the structure of cisplatin, which consists of a central charged platinum ion surrounded by four ligands; two amine ligands and two chloride ligands. The amine ligands have a stronger bond with the platinum, which allows the chloride ions to form leaving groups once inside the cell and so the platinum can interact with DNA bases, causing the formation of lesions<sup>3</sup>.

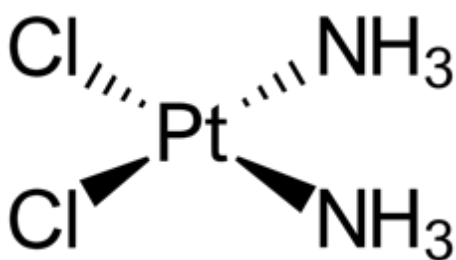


Figure 1.1: Cisplatin molecular structure <sup>4</sup>

Cisplatin is a widely used form of chemotherapy for a number of cancers including bladder, testicular, head and neck, breast, stomach and prostate cancers amongst others. Despite being a first line treatment option for many cancers with a high initial response rate of over 70%<sup>5</sup>, cisplatin can cause many harmful side effects. Cisplatin is

given intravenously so it is taken directly into the bloodstream and can reach tumor cells rapidly. It is taken up into cells via passive diffusion<sup>6</sup> and as it cannot distinguish between dividing cancer cells and normal cells, it exhibits equal toxicity on both. Despite being a common form of treatment, cisplatin can cause various complications including nephrotoxicity and ototoxicity<sup>7</sup>.

### **1.3 Brain cancer**

Brain cancer is a relatively rare form of cancer, making up approximately 2-3% of all cancer cases in the UK. However, brain tumour incidence rates are predicted to increase by 6% in the UK by 2035, as shown in the graph in **figure 1.2**. These statistics indicate brain tumors are becoming a greater problem<sup>8</sup>. There are many different types of brain cancer and they are given a grade between 1 - 4 depending on how serious they are. Grade 1 and 2 indicate slower growing, less severe tumors whereas grades 3 and 4 are indicative of fast growing, malignant tumors which are harder to treat. Brain tumors can be classified as primary or secondary tumors, depending on their origin. Primary tumors arise from cells within the brain whereas secondary tumors are those which have been caused by metastasis, the movement of malignant cells from other areas of the body to the brain.

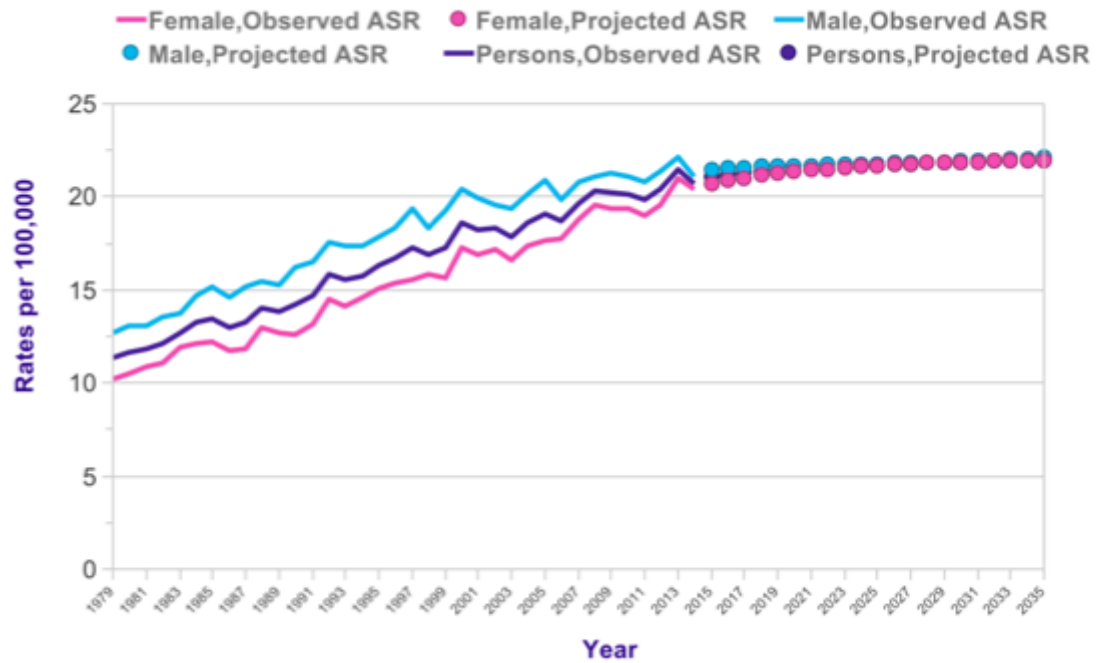


**Fig 1.2: Observed and projected age standardized incidence rates of Brain cancer, by sex, UK 1979-2035.** (Cancer Research UK)<sup>8</sup>

The most common type of brain tumor is a glioma, which originates in the glial tissue of the nervous system. These can be categorized according to which type of cell they arose from. Oligodendroglioma is a less common form of glioma making up only about 3% of brain tumors<sup>9</sup>. They originate from oligodendrocytes which are responsible for producing the myelin sheath which surrounds nerves and helps speed up the transmission of nerve signals<sup>10</sup>. The least common type of glioma is an ependymoma, which originates in ependymal cells, these cells form an epithelial layer which acts as a barrier between the ventricles containing cerebrospinal fluid (CSF) and the central canal of the spinal cord<sup>11</sup>.

Astrocytomas are a type of glioma which are derived from astrocytes, important cells in the nervous system which support the blood-brain barrier, provide nutrients to neurons and repair damaged nervous tissue. A grade 4 astrocytoma is also known as a glioblastoma, or glioblastoma multiforme (GBM), the most aggressive type of brain tumour.

Whilst the outlook for patients with a low grade glioma is relatively positive, those with more advanced grades of glioma have very low rates of survival. According to Cancer Research UK, people with a grade 1 astrocytoma have over 90% chance of survival for 5 years or more. However, those with grade 4 astrocytoma, or GBM, have a poor prognosis with only 5% of patients surviving 5 years or more<sup>12</sup>.

### **1.3.1 Brain cancer: Symptoms**

Brain tumors can be identified through a number of different physical symptoms. These include headaches which are caused by pressure placed on brain matter due to the growth and swelling of the tumor. Other signs include alterations in function, such as decreased function in the right side of the body due to damage in the left side of the brain. Extreme pressure on the neurons in the brain may trigger seizures, characterized by the twitching of one or more limbs followed by potential paralysis.

### **1.3.2 Brain cancer: Diagnosis**

A doctor can confirm the presence of a brain tumour by conducting a computerized tomography (CT) or magnetic resonance imaging (MRI) scan to examine the brain tissue and detect any abnormal growth. A doctor may also conduct a biopsy in which a small section of the tumour tissue is removed and examined to determine the origin and stage of the tumour, further treatment can then be arranged depending on the seriousness of the tumour.

### **1.3.3 Brain cancer: Treatments**

Current treatments for brain cancer include surgery, radiotherapy and chemotherapy. The primary form of treatment for gliomas is surgery in which a highly trained surgeon performs a craniotomy in an attempt to remove as much of the tumour as possible. It is a common occurrence for some of the tumour to remain after surgery in which case the patient will need to undergo further treatments such as chemotherapy or radiotherapy. Steroids are often given to patients in order to relieve symptoms as they are able to decrease the swelling in the brain which can cause significant damage<sup>13</sup>.

Whilst surgery is the initial treatment option for the majority of glioblastoma patients, it is a risky procedure, as the brain tissue is very important for human function, if any of the healthy, non-tumor tissue is removed or damaged, this may impair some vital functions such as speech or movement. To enhance the precision of craniotomy procedures, a fluorescent marker was developed called 5- Aminolevulinic acid (5-ALA)

which was approved by the US Food and Drug Administration (FDA) for use on high grade gliomas<sup>14</sup>. This is informally known as the 'pink drink' as it is ingested orally by a patient prior to surgery. This compound can be taken up by brain cells and in high grade glioma cells is metabolized into a fluorescent product protoporphyrinogen IX (PpIX), which fluoresces red when exposed to blue light of a certain wavelength. This process only occurs in high grade glioma tumor cells and so the accumulation of PpIX allows them to be distinguishable from normal brain matter<sup>15</sup>. This allows 5-ALA to be used as a tumor visualizing agent to aid in locating the tumor during brain surgery, whilst reducing the likelihood of damage to healthy areas of the brain. Although 5-ALA has proven to be a useful surgical aid, it can only be used on high grade gliomas which are more advanced and generally have poorer prognosis, suggesting the need for a fluorescent marker which can be used on low grade brain tumors as this could increase the chance of patient survival.

Radiotherapy is often required if a patient has undergone surgery but not all the tumor has been removed. Targeted radiation can remove any traces of cancerous cells and has been shown to prolong survival in glioblastoma patients from 14 weeks to 36 weeks<sup>16,17</sup>. Radiation normally successfully results in a period of remission but unfortunately most patients experience a relapse of the tumor within a year following treatment.

One of the existing first line treatments for advanced glioblastoma is the drug temozolomide, an alkylating agent which is active during the resting phase of the cell. Temozolomide works by methylating bases on DNA, mainly at the N7 position of guanine, the O3 position of adenine and the O6 position of guanine<sup>18</sup>. This causes DNA damage, thus inhibiting DNA replication and inducing cell cycle arrest, so the cells are unable to divide<sup>18</sup>. This eventually results in apoptosis and so depletion of the tumour. Temozolomide has shown to be effective at treating brain tumors and can increase the average survival of patients, with one study finding that two-year survival rate was 10.4% with just radiotherapy versus 26.5% when patients were treated with temozolomide alongside radiotherapy<sup>20</sup>. However, over 50% of glioblastoma tumors are able to produce O6-methylguanine-DNA methyltransferase (MGMT), a protein with DNA repairing properties which renders temozolomide ineffective<sup>21</sup>.

Another common form of chemotherapy used for glioblastoma patients is Bevacizumab (Avastin), a type of drug called a monoclonal antibody which acts as an anti-angiogenesis drug and targets vascular endothelial growth factor (VEGF) on the cell membrane, thus starving the tumor of oxygen so it is unable to grow.

#### **1.4 Chemotherapy**

Although some drugs currently available such as temozolomide and cisplatin are usually effective at treating tumors, chemotherapy in general poses a problem as it is unable to differentiate between cancerous cells and normal healthy cells which have

high proliferation, such as skin fibroblasts and hair cells. As a consequence, normal cells are targeted and destroyed. This can result in serious side effects, such as hair loss, fatigue, nausea and vomiting, which cause pain and distress to the patient. A possible solution to this issue would be to develop a new form of therapy which specifically targets tumor cells so that other cells in normal tissue in the body do not suffer as a result. Alternatively, the development of a method to increase the efficacy of chemotherapy would be an ideal solution to enhance existing cancer treatments whilst reducing their toxicity on other, healthy areas of the body.

Compounds which are able to identify and bind cancer cells selectively are the next step in improving cancer treatment. This issue is particularly important in brain tumors as the tissue is delicate and surgical procedure can go wrong so requires very precise removal. If, during surgery, any extra non-cancerous tissue is removed this may result in serious brain damage and loss of function.

### **1.5 Novel antimicrobial compounds**

A number of new compounds have been generated by Dr. Jennifer Hiscock at the University of Kent which were named supramolecular self-associating antimicrobials (SSAs). These compounds are toxic on both gram positive (MRSA) and gram negative (*E. coli*) bacteria and are thought to exert anti-cancer activity due to the similarities in composition between bacterial cell membranes and cancer cell membranes. Over 50 variations of these compounds were screened against MRSA and *E. Coli* through drop

testing methods and growth rate methods, and the findings have been published and registered as a patent (No. PCT/EP2018/069568). The exact mode of action of these compounds is not yet fully understood, however they are believed to interact with the lipid component of the cell surface membrane, and once they accumulate in high enough concentrations on the cell membrane it is believed they are able to form structures through self-association methods and then enter the cell and interact with intracellular components.

These novel compounds are sulfonate-urea based amphiphilic salts, meaning they possess both hydrophilic and hydrophobic properties, as shown in **figure 1.3**. The hydrophilic end of the compound has hydrogen bond accepting (HBA) function, and these compounds also contain a region which has both hydrogen bond accepting and hydrogen bond donating (HBD) functionalities. The general structure of these compounds also incorporates an aromatic ring structure, usually trifluoromethyl benzene. These compounds are accompanied by a counter cation which provides a positive charge. The main counter cation used is tetrabutyl ammonium (TBA), but there are some variations that are used such as tetra methyl ammonium (TMA) and tetra propyl ammonium (TPA).

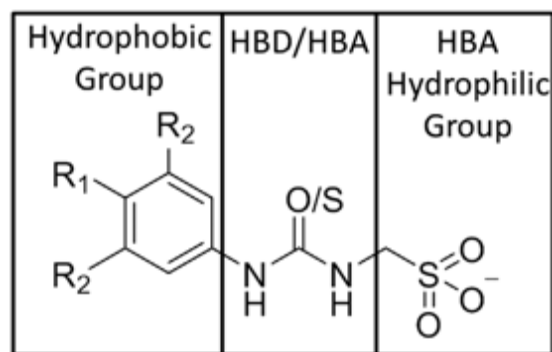


**Figure 1.3: General structure of novel amphiphilic compounds.**<sup>22</sup>

These amphiphilic compounds are able to self-associate through the formation of hydrogen bonds, in a number of different configurations. The compounds were examined using x-ray crystallography to produce 3D images of the dimer formation. This provided an insight into the structure of the monomers and the bonds they form to result in dimers, an example of which is shown in **figure 1.4**. In this model, the amine group acts as the hydrogen bond donor whilst the oxygen groups on the sulfur atom are the hydrogen bond acceptors. These compounds can form a dimer through the formation of four hydrogen bonds. The compounds were shown to be able to adopt multiple hydrogen bonding modes at the same time. This allows them to form structures on the cell surface membrane where they can potentially associate with and pass through the membrane.

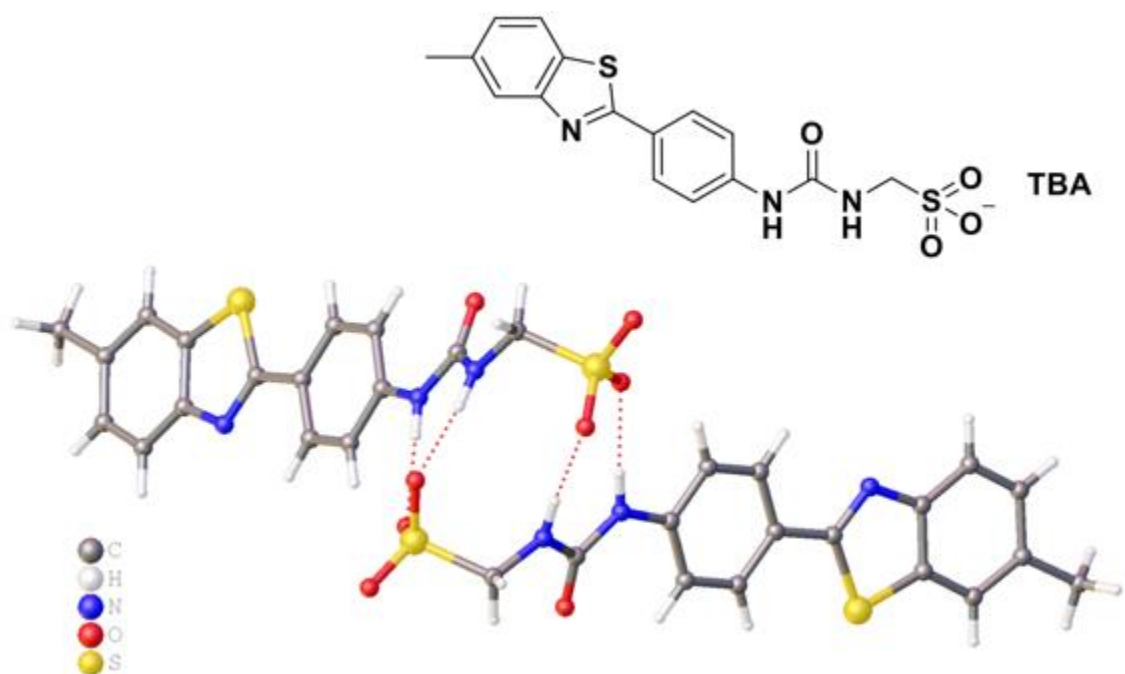


**Figure 1.4: Molecular structure of fluorescent compound 31, and below a single crystal X-ray structure of this compound in dimer form, through urea-anion complex formation<sup>22</sup>.**

The development of intrinsically fluorescent SSAs allowed the study of their activity on a cellular level, the compounds were analyzed using transmission and fluorescence microscopy to understand their mode of action. These experiments demonstrated the formation of circular structures, or aggregates, in the solution state<sup>23</sup>. Several of these microscopy experiments showed the compounds selectively bound to microbes and formed ring like structures around the membrane of the cells. The fluorescence experiments revealed that the compounds interact with the bacterial cell membranes, and that they appear have a greater association with the membranes of *S. aureus* than with *E. coli*.

### 1.5.1 Compound structure

Compounds looked at in this project were compounds 1 (1-25), 3 (1-3-O), 9 (1-20), 11 (1-18), 14 (KN2A), 30 and 31 (2-35). The structures of which can be found in **figure 1.5** below.

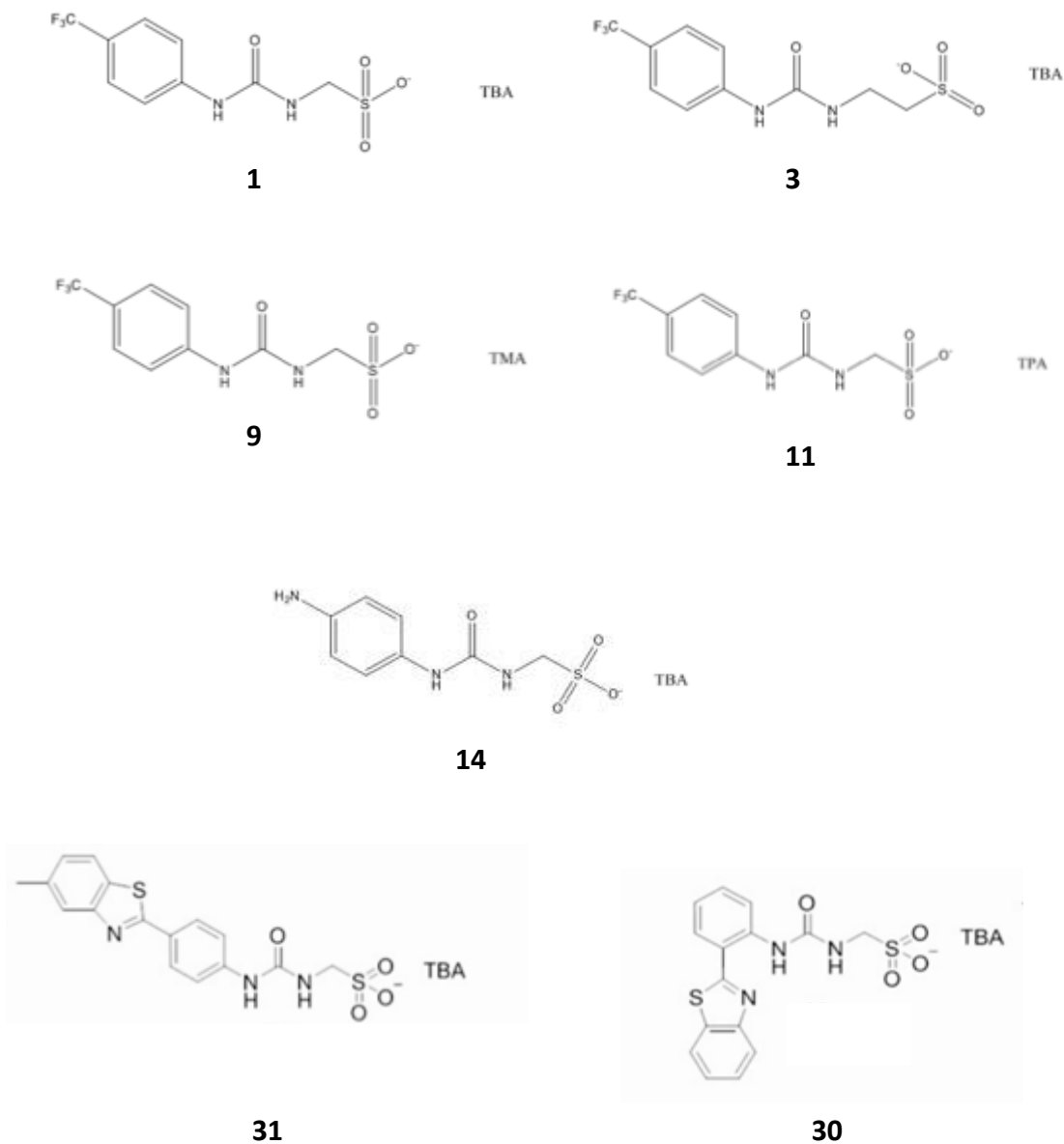


**Figure 1.5: Molecular structures of the series of compounds selected for mammalian testing in this project** shown above: Compound 1 (1-25), Compound 3 (1-3-O), Compound 9 (1-20), Compound 11 (1-18), Compound 14 (KN2A) and fluorescent Compounds 30 and 31

## **1.6 Composition of cancer cells compared to normal cells**

A notable feature of tumor cells is they often have an acidic extracellular environment, this is due to the tendency of cancer cells to produce energy through glycolysis as opposed to oxidative phosphorylation, which is a much more efficient method of ATP production. Cancer cells opt for this pathway even when sufficient levels of oxygen are present, and this results in an excessive production of lactate – also known as the Warburg effect<sup>24</sup>. In contrast, normal healthy cells generally have a neutral or slightly positively charged extracellular environment, as they favor oxidative phosphorylation as a method of ATP production, and so there is no acidic byproduct.

## **1.7 Membrane lipid composition**

Polar phospholipids, such as phosphatidylethanolamine (PE) and phosphatidylserine (PS), are normally contained in the inner layer of the membrane bilayer in normal human cells whilst the outer layer tends to have a higher prevalence of zwitterionic lipids such as phosphatidylcholine (PC) and sphingomyelins. This asymmetric organization of membrane lipids is sustained by various enzymes such as flippases, translocases and scramblases<sup>25,26</sup>. However, in cancerous cells the polar lipids have a tendency to switch to the outer layer of the phospholipid bilayer, and so negatively charged lipid groups are presented on the cell surface membrane of tumor cells<sup>27</sup>, resulting in a negatively charged extracellular environment.

Similarly, bacteria also exhibit a negatively charged extracellular environment, bacterial cell membranes are normally composed of lipids such as phosphatidylglycerol and

cardiolipin, with phosphatidylethanolamine being the main constituent – PE constitutes approximately 75% of membrane lipids in *E. coli*. Bacterial membranes may also contain phosphatidylcholine and phosphatidylinositol, but these lipids are generally more abundant in eukaryotic cells. The hypothesis is therefore that the SSA compounds are able to bind negatively charged membrane lipids and disrupt the cell membrane through pore formation or cell lysis.

### **1.8 Differential membrane composition of brain tumour cells**

Studies using desorption electrospray ionization mass spectrometry (DESI-MS) imaging have shown that the composition of the cell membrane of normal brain cells differs from those of brain tumor cells<sup>28</sup>. This difference in membrane structure is likely due to mutations in the isocitrate dehydrogenase (IDH) 1 gene. IDH1 is an enzyme located in the cytoplasm which is responsible for catalyzing the oxidative decarboxylation of isocitrate to alpha-ketoglutarate outside of the krebs cycle. The mutated form causes them to produce 2-hydroxyglutarate instead of its normal product NADPH.

Mutations in IDH1 have been identified in approximately 80% of grade 2 and 3 gliomas and secondary glioblastoma multiforme (GBM)<sup>29</sup>. IDH1 mutations are caused by a singular heterozygous missense amino acid at arginine residue 132<sup>30</sup>. This residue is part of the active site of the enzyme so a change in amino acid structure has a critical effect on substrate binding of isocitrate, so it cannot perform its usual catalytic activity<sup>31</sup>.

The theory proposed by Dr. Hiscock is that the differential lipid composition of tumor cells will allow these newly developed amphiphilic molecules to selectively bind to cancer cells through the formation of non-covalent interactions. The compounds are able to differentiate between the cancerous cells and normal healthy cells so this could be a potential new form of targeted therapy for cancer.

### **1.9 Project aims**

The primary aim of this research project were to investigate whether these new SSA compounds have a biological effect on human cancer cell lines. The cell lines used in this study were the U87MG human glioblastoma cell line of epithelial origin and A2780, a human ovarian carcinoma cell line.

The main objectives were:

- To determine if any of the series of compounds have an effect on growth of cancer cells through SRB analysis.
- To investigate whether these SSA compounds are able to bind to and/or enter cancer cells, using fluorescence microscopy.
- Explore the hypothetical use of these compounds as drug delivery systems as they are thought to be able to self-associate and form aggregates in solution so they could potentially be used as a delivery system if they preferentially bind cancerous cells.

Using various experimental methods, I will aim to produce a set of results to support the hypothesis regarding these novel compounds and provide some insight into their potential as a new form of cancer therapy.

## **2. Materials and Methods**

### **2.1 Cell Lines**

Cell lines used were U87MG of human glioblastoma origin and A2780 human ovarian carcinoma of epithelial origin. Both obtained from the Institute of Cancer Research UK (ICR).

### **2.2 Compounds**

All of the SSA compounds used in this project were obtained from the Hiscock lab. They were dissolved in 5% ethanol at a stock concentration of 20mM. Compound stocks were stored at -20°C and thawed before use.

### **2.3 Cell culture**

U87MG and A2780 cells were cultured in Iscove's Modified Dulbecco's Medium (IMDM) supplemented with 10% Fetal bovine serum (FBS). Cells were cultured at optimum conditions of 37°C and 5% CO<sub>2</sub>.

To split the cells, old media was removed from the T25 flasks containing cells, and any remaining media was washed off using ~1ml phosphate buffered saline (PBS). Cells were detached from flasks using ~0.5ml Trypsin EDTA x10 solution and then resuspended in 5ml fresh media. Approximately 0.5 – 2 mls of this new cell solution was transferred to a new T25 flask and resuspended in 5mls fresh media. Cell were split every 3-4 days, depending on when they reached 70% confluency.

## **2.4 Cell Seeding Density assays**

To determine the optimum growth density of the cell lines, cells were plated in 96 well format at a range of concentrations and grown over a period of 168 hours to measure growth. U87MG cells were plated at densities ranging from 12,800 cells per well to 800 cells per well with PBS in outer wells to prevent evaporation of media. A2780 cells were plated at concentrations ranging from 3200 cells per well to 200 cells per well. Seven identical plates were made up and incubated at 37°C and 5% CO<sub>2</sub>. One plate was stopped every 24 hours and fixed with 70µl 10% trichloroacetic acid (TCA) for 30 mins, then washed in distilled water 5 times and 70µl sulfurdhodamine B (SRB) dye was added for 30 mins at room temperature and then the plate was washed with 1% acetic acid and dried in a 37°C oven overnight. Once all seven plates were fixed and stained, they were put on a shaker for 10 mins at 200rpm with 100µl of 10 mM Tris buffer in each well to solubilize the dye. Plates were then read at 490nm on a Victor X4 plate reader, results analyzed using GraphPad Prism.

## **2.5 SRB assays**

Once the optimum cell density was determined, the cells were plated in 96-well plates and treated with a range of concentrations of each compound after 48 hours. Plates were then incubated at 37°C and 5% CO<sub>2</sub> for a further 96 hours after which they were removed, fixed using 10% TCA and stained using SRB dye. 10mM Tris buffer was added to each well and plates were shaken for 10 mins at 200rpm. Plates were then read at 490nm on a Victor X4 plate reader, results analyzed using GraphPad Prism to

produce a viability curve and produce an IC<sub>50</sub> value. The IC<sub>50</sub> is the concentration of drug at which the SRB signal is reduced by 50% over the time course of the assay.

## **2.6 Combination studies**

### **2.6.1 Chou-Talalay assay**

Drug combinations were studied using the Chou-Talalay method in which different titrations of Cisplatin in combination with either Compound 1 or 31 were tested on A2780 cells and levels of synergy were calculated using Compusyn software.

Compound 1/31 and Cisplatin combination was tested using this method. Cells were plated at 800 cells per well and incubated for 48 hours. Compound 1/31 was added 1 hour prior to Cisplatin at a concentration range of 40 $\mu$ M – 1.25 $\mu$ M, with Cisplatin at a range of 2.4 $\mu$ M – 0.075 $\mu$ M. Compound/ Cisplatin were added to the plate to form a matrix of different concentrations. Cells were incubated with the drugs for 96 hours and then fixed and stained using SRB dye, and the absorbance read at 490nm. Data was analyzed using Microsoft Excel and then input in to Compusyn software for analysis.

### **2.6.2 Combination assay**

Drug combinations were further explored using another assay allowing lower concentrations of Compound 1 to be investigated. Compound 1 was used at various concentrations of the IC<sub>50</sub>, these were the IC<sub>10</sub> ( $\mu$ M), IC<sub>5</sub> (4 $\mu$ M), IC<sub>2.5</sub> (2 $\mu$ M), IC<sub>1</sub> (0.8 $\mu$ M) and the IC<sub>0.25</sub> (0.2 $\mu$ M). A2780 cells were plated at 800 cells per well in 96 well plates,

and treated with compound 1 an hour before addition of Cisplatin. Cisplatin range was 2.4 $\mu$ M – 0.075 $\mu$ M. Plates were then incubated for 96 hours before being fixed and stained with SRB as described previously. Data was analyzed using Microsoft Excel and graphs produced using GraphPad Prism.

## **2.6 Immunofluorescence**

A2780 cells were plated at ~750,000 cells per dish and U87MG cells were plated at ~600,000 cells per dish in glass bottomed 3cm dishes for live cell imaging. Compound 31 was added at a concentration of 90 $\mu$ M after 24 hours incubation at 37°C, 5% CO<sub>2</sub>. Compound 30 was added at a concentration of 180 $\mu$ M after 24 hours incubation at 37°C, 5% CO<sub>2</sub>. Samples were examined after an hour exposure to the compound, an immediate exposure and an untreated control.

## **2.7 Western Blot analysis**

A2780 cells were plated at ~ 1,000,000 cells in 10cm dishes. Cells were left for 48 hours and then treated with varying concentrations of compound 1 and cisplatin. Different combinations of drug treatment were used to represent high and low concentrations.

High Cisplatin: 10 $\mu$ M

Low Cisplatin: 1 $\mu$ M

High Compound 1: 400 $\mu$ M

Low Compound 1: 40 $\mu$ M

The cells were left in drug for 24 hours and then stopped by washing with ice cold PBS. Plates were lysed and scraped for 30 minutes on ice with 100µL lysis buffer. Lysate was collected in eppendorfs and centrifuged to form a cell pellet. The supernatant was removed from each sample and the concentration of protein in each sample was calculated using the Bradford assay. Samples were then normalized to an equal concentration using lysis buffer, and 12.5 µL 4x sample buffer was added to each sample. The samples were then mixed and heated at 95°C for 5 minutes before being run on a poly acrylamide gel.

Samples were run on a 12% gel in order to allow detection of different sized protein targets. Electrophoresis was run at 150V for approximately 1 hour. Proteins were then transferred to a PVDF membrane through wet transfer at 100V for 90mins. To ensure all protein had transferred, membranes were stained with Ponceau S. After protein transfer, the PVDF membrane was blocked in 5% milk in 0.1% TBST for 1 hour.

Membrane was then cut at the appropriate molecular weight sites and incubated in primary antibody (See **table 2.1** for list of antibodies used) in 5% milk overnight at 4°C (Gamma H2AX antibody incubated in 5% BSA in 0.1% TBST). The following day, membranes were washed 4 x 5 minutes with 0.1% TBST and then incubated with HRP-conjugated secondary antibody in 5% milk for 1 hour at room temperature.

Membranes were then washed 4 x 5 minutes in 0.1% TBST before being treated with ECL reagent for 5 mins and then exposed to Amersham hyperfilm in a dark room. The film was developed in an optimax 2010 developer.

**Table 2.1: List of antibodies used for western blot analysis**

<b>Primary antibody</b>	<b>Supplier</b>	<b>Catalogue number</b>	<b>Species</b>	<b>Dilution</b>
AKT	Cell signalling	4691	Rabbit	1:5000
AKT pSer473	Cell signalling	4060	Rabbit	1:1000
ERK 1/2	Cell signalling	4695	Rabbit	1:1000
ERK1/2 pT202/Y204	Cell signalling	4370	Rabbit	1:2000
CDK1	Santa Cruz	sc-8395	Mouse	1:2000
CDK1 pTyr15	Cell signalling	9111	Rabbit	1:1000
Chk1	Cell signalling	2360	Mouse	1:1000
Chk1 pSer296	Cell signalling	2349	Rabbit	1:1000
PARPC	Cell signalling	9541	Rabbit	1:1000
p21	Cell signalling	2947	Rabbit	1:1000
Gamma H2AX	Cell signalling	05-636	Mouse	1:500
GAPDH	Millipore	MAB374	Mouse	1:100,000
<b>Secondary antibody</b>	<b>Supplier</b>	<b>Catalogue number</b>	<b>Species</b>	<b>Dilution</b>
Anti-mouse HRP conjugate	Bio-Rad	170-6516	Goat	1:10,000
Anti-rabbit HRP conjugate	Bio-Rad	170-6515	Goat	1:10,000

**Table 2.2: List of buffers used for western blot analysis**

<b>Lysis Buffer</b>	50 mM HEPES pH 7.4, 250 mM NaCl, 0.1% Nonidet-P40, 1 mM DTT, 1 mM EDTA, 1 mM NAF, 10 mM $\beta$ -glycerophosphate, 0.1 mM sodium orthovanadate, and Complete™ protease inhibitor cocktail [Roche, Switzerland]
<b>SDS-PAGE Running buffer</b>	<b>10X:</b> 0.25M Tris-HCl, 1.92M Glycine, 1% SDS in dH <sub>2</sub> O <b>1X:</b> 100mL 10X solution, 900mL dH <sub>2</sub> O
<b>Transfer buffer</b>	<b>10X:</b> 0.25M Tris-HCl, 1.92M Glycine in 1L dH <sub>2</sub> O <b>1X:</b> 100mL of 10X solution, 100mL methanol, 800mL dH <sub>2</sub> O
<b>TBS</b>	<b>10X:</b> 50mM Tris-HCl, 150mM NaCl in dH <sub>2</sub> O (pH 8) <b>1X:</b> 100mL 10X TBS, 900mL dH <sub>2</sub> O
<b>Washing buffer (0.1% TBST)</b>	1 ml Tween 20 dissolved in 1L 1X TBS Stored at room temperature
<b>Blocking buffer</b>	5% Marvel milk powder dissolved in 1X TBST. Use immediately or store at 4°C for up to 24 hours.
<b>Stripping Buffer</b>	50mM Glycine, 1% SDS in dH <sub>2</sub> O (pH 2)

### 3. Results

#### 3.1 Cell lines

Two human cell lines were used in this project; A2780 ovarian endometroid adenocarcinoma and U87MG glioblastoma cell lines. Images were taken of these cells in culture to see the morphology and growth characteristics of each cell line as shown in **figure 3.1 and 3.2** below. Images were taken at high and low density. Both A2780 and U87MG are adherent cell lines with epithelial morphology, and grow as a monolayer in tissue culture flasks.

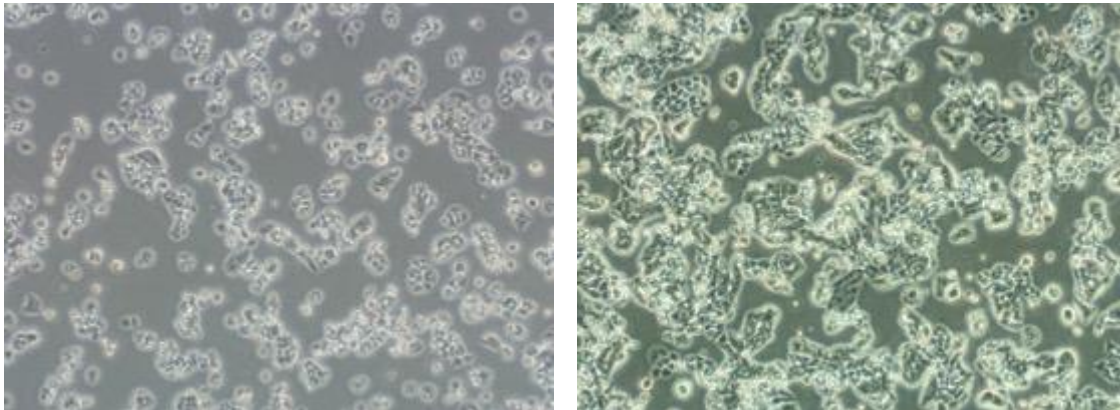


**Figure 3.1: Microscope images of A2780 cells in culture.** Cells growing in IMDM media + 10% FBS. Low density (left) and high density (right), taken at 40x magnification on a bright field microscope.

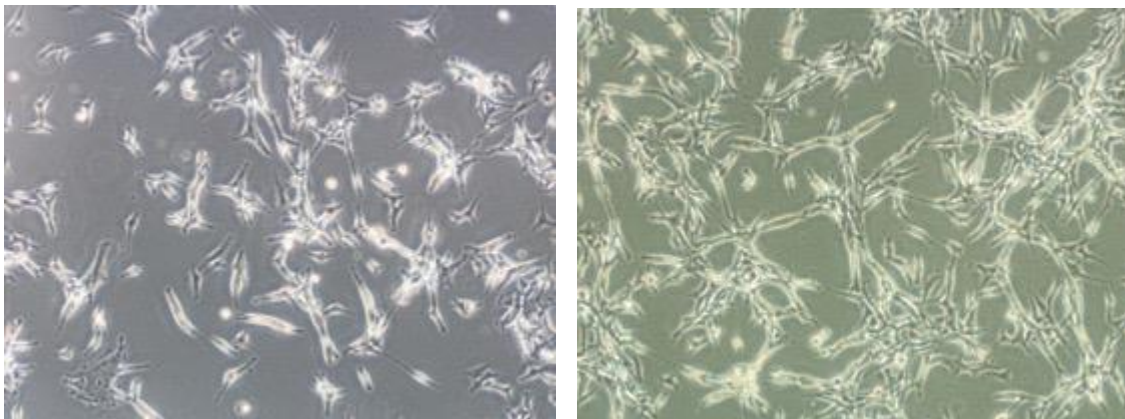


**Figure 3.2: Microscope images of U87MG cells in culture.** Cells growing in IMDM media + 10% FBS. Low density (left) and high density (right), taken at 40x magnification on a bright field microscope.

### 3.2 Cell density seeding assay

To determine the optimal seeding density for each cell line, a seeding density assay was conducted with 5 different densities and the ideal cell density for a 96-well plate was decided from the best growth curve. The ideal curve would have the cells in logarithmic growth throughout the 96-hour timeframe of an assay. The curves were also used to calculate the doubling time for each cell line. The growth curves are shown in **figure 3.3** and **3.4**, these are representative of 4 biological repeats.

#### 3.2.1 Doubling time calculation

Doubling time of cell lines was calculated using the equation below<sup>32</sup>:

$$DoublingTime = \frac{duration * \log(2)}{\log(FinalConcentration) - \log(InitialConcentration)}$$

### 3.2.2 A2780 Seeding Density

For the A2780 ovarian carcinoma cell line, the optimum cell seeding density was determined to be 800 cells per well (cpw) using the graphs in **figure 3.3**. The doubling time was calculated to be approximately 15 hours.

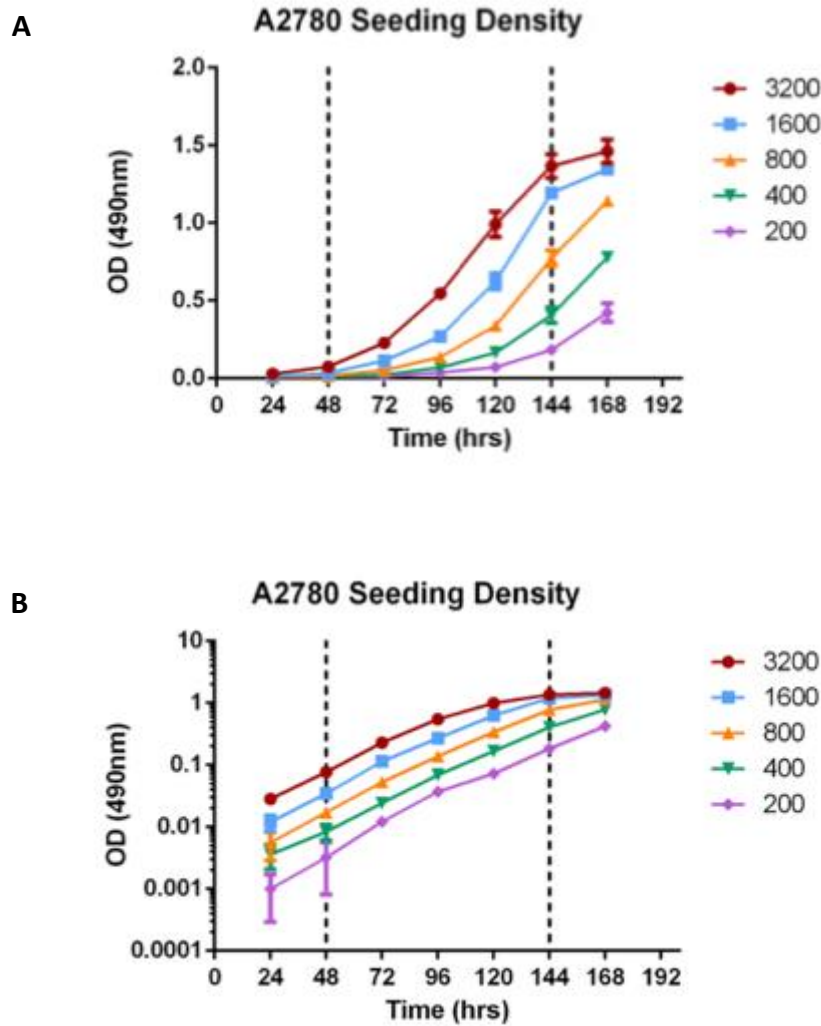


**Figure 3.3: Cell seeding density graph on linear scale (A) and logarithmic scale (B) for A2780 ovarian carcinoma cell line.** Cells plated at 5 different densities (200 cpw – 3200 cpw) and absorbance measured at 490nm at 24 hour intervals for 168 hours. (Data represents n=4 individual experiments)

### 3.2.3 U87MG Seeding Density

For the U87MG glioblastoma cell line, the optimum cell seeding density was determined to be 6400 cells per well using the graphs in **figure 3.4**. The doubling time was calculated to be approximately 32 hours.

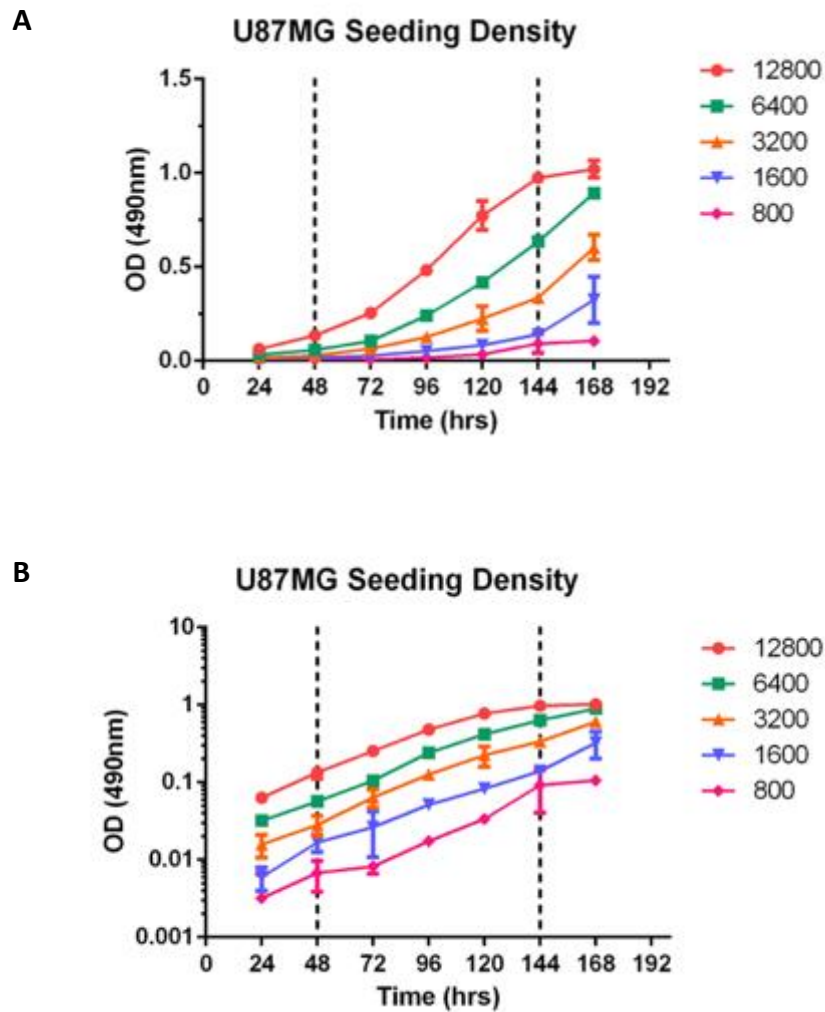


**Figure 3.4: Cell seeding density graph on linear scale (A) and logarithmic scale (B) for U87MG glioblastoma cell line.** Cells plated at 5 different densities (800 cpw – 12800 cpw) and absorbance measured at 490nm at 24 hour intervals for 168 hours. (Data represents n=4 individual experiments)

### 3.3 Toxicity assay and IC<sub>50</sub> determination

Toxicity of SSA compounds was determined using a 96 hour Sulfurhodamine B (SRB) assay. Both A2780 and U87MG cell lines were treated with a range of concentrations for each compound (1, 3, 9, 11, 14, 30, 31) and Cisplatin was used as a control. After 96 hours, the assay was stopped and the absorbance was read at 490nm. The absorbance values were used to calculate the percentage growth compared to the untreated control. These were then plotted in GraphPad Prism to obtain a growth curve and calculate an IC<sub>50</sub> value. IC<sub>50</sub> is defined as the concentration at which 50% of growth is inhibited. IC<sub>50</sub> values of each compound on both cell lines are shown in **Table 3.1** below, values are the mean of 3 biological repeats with standard deviation.

**Table 3.1:** Summary of IC<sub>50</sub> data of A2780 cells and U87MG cells treated with compound 1, 3, 9, 11, 14, 30, 31 and Cisplatin control. All values expressed in  $\mu\text{M}$  with standard deviation. Each value is representative of 3 separate biological repeats.

Compound	A2780 ( $\mu\text{M}$ )	U87MG ( $\mu\text{M}$ )
<b>1</b>	44.61 $\pm$ 18.5	248 $\pm$ 21.9
<b>3</b>	53.57 $\pm$ 16.8	316 $\pm$ 49.1
<b>9</b>	277.94 $\pm$ 18.2	394.6 $\pm$ 99.5
<b>11</b>	451.33 $\pm$ 38.3	>500
<b>14</b>	51.28 $\pm$ 16.5	297.3 $\pm$ 92.3
<b>30</b>	59.53 $\pm$ 8.1	367.3 $\pm$ 48.5
<b>31</b>	29.61 $\pm$ 9.7	188.98 $\pm$ 51.8
<b>Cisplatin</b>	0.79 $\pm$ 0.4	6.41 $\pm$ 4.7

The growth curves of each compound on both A2780 and U87MG cell lines are shown in **figure 3.5** and **3.6** below. The dotted line indicates where the growth of cells is at

50% compared to the untreated control, these were used to calculate the IC<sub>50</sub> value for each compound. From looking at this datum, it is clear that all of the selected SSA compounds have a toxic effect on both A2780 and U87MG cells, with some being more effective than others. The IC<sub>50</sub> values indicate that compound 31 is the most effective compound at killing both A2780 and U87MG cells, exhibiting IC<sub>50</sub> values of 29.61 ± 9.7 and 188.98 ± 51.8 respectively. Compound 11 was the least toxic compound on both cell lines, with an IC<sub>50</sub> value of 451.33 ± 38.3 on A2780 cells. As shown in **figure 3.6**, the growth curve for compound 11 was unable to cross the 50% line, indicating compound 11 could not kill 50% of the population even at the highest concentration (500µM) so an IC<sub>50</sub> value could not be calculated for compound 11 on U87MG cells. The order of their toxicity had the same trend across both cell lines. The order from most to least effective is as follows:

$$31 > 1 > 14 > 3 > 30 > 9 > 11$$

Looking at the growth curves in **figure 3.5** and **3.6** and **table 3.1**, it seems A2780 cells are more sensitive to these compounds as the IC<sub>50</sub> values for all the compounds and cisplatin are higher for U87MG cells. However, it should be noted that the vast differences in IC<sub>50</sub> values between the two cell lines are likely due to the difference in seeding densities used. The seeding density used for U87MG was 6400cpw which is 8 times that of the seeding density for A2780 (800 cpw). Looking at the IC<sub>50</sub> values of each compound, they appear to reflect this difference as all the values for U87MG are approximately 8 times as much as the values for A2780.

### 3.3.1 Toxicity graphs of each compound on A2780 cells

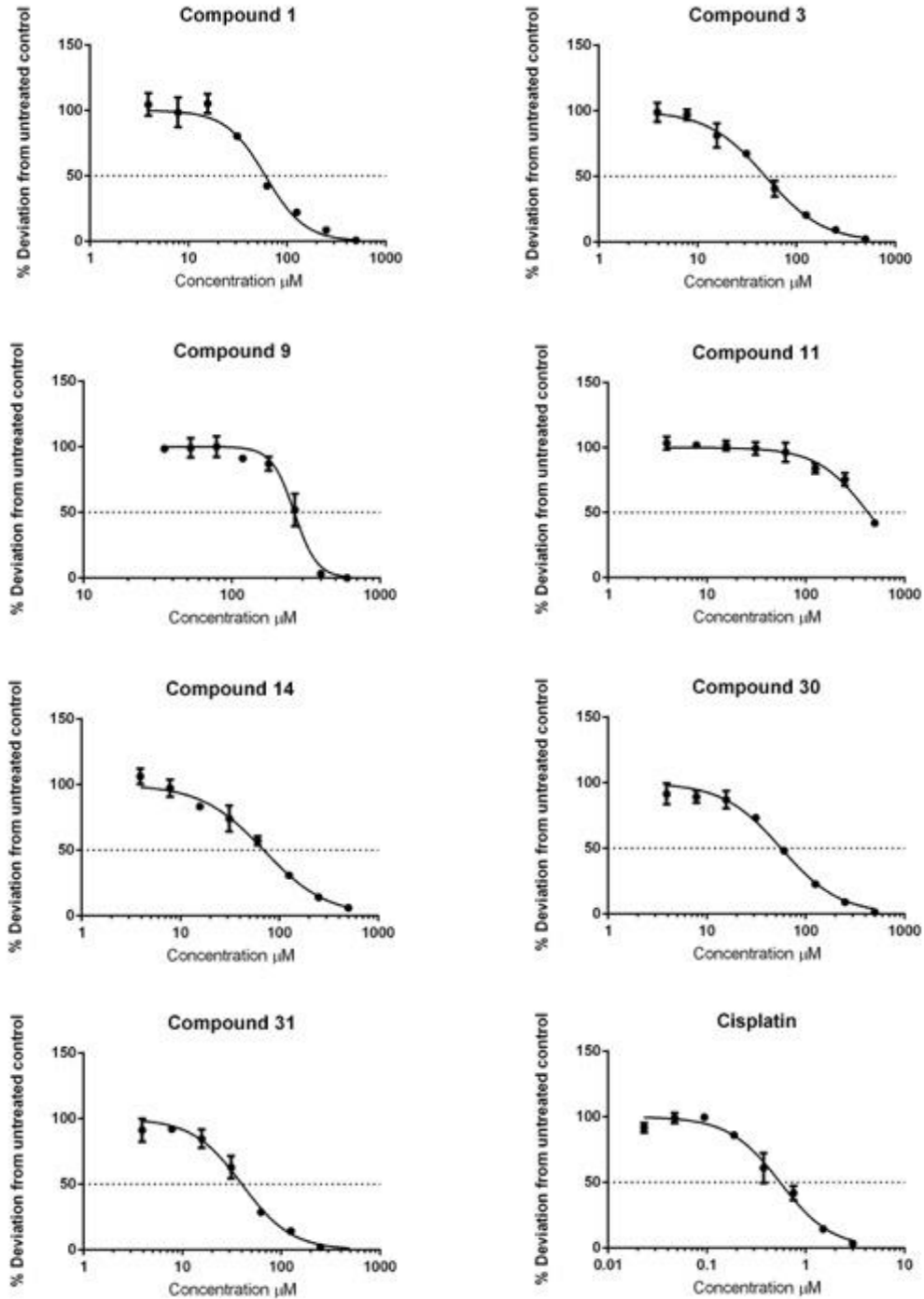


**Figure 3.5: Cell viability curves of A2780 cells treated with Compound 1, 3, 9, 11, 14, 30, 31 and Cisplatin for 96 hours.** Growth determined through SRB assay. Cells seeded at 800 cpw and treated with compound after 48 hours. Plates left for further 96 hours, stopped and absorbance measured at 490nm. Data represents n=3 separate experiments.

### 3.3.2 Toxicity graphs of each compound on U87MG cells

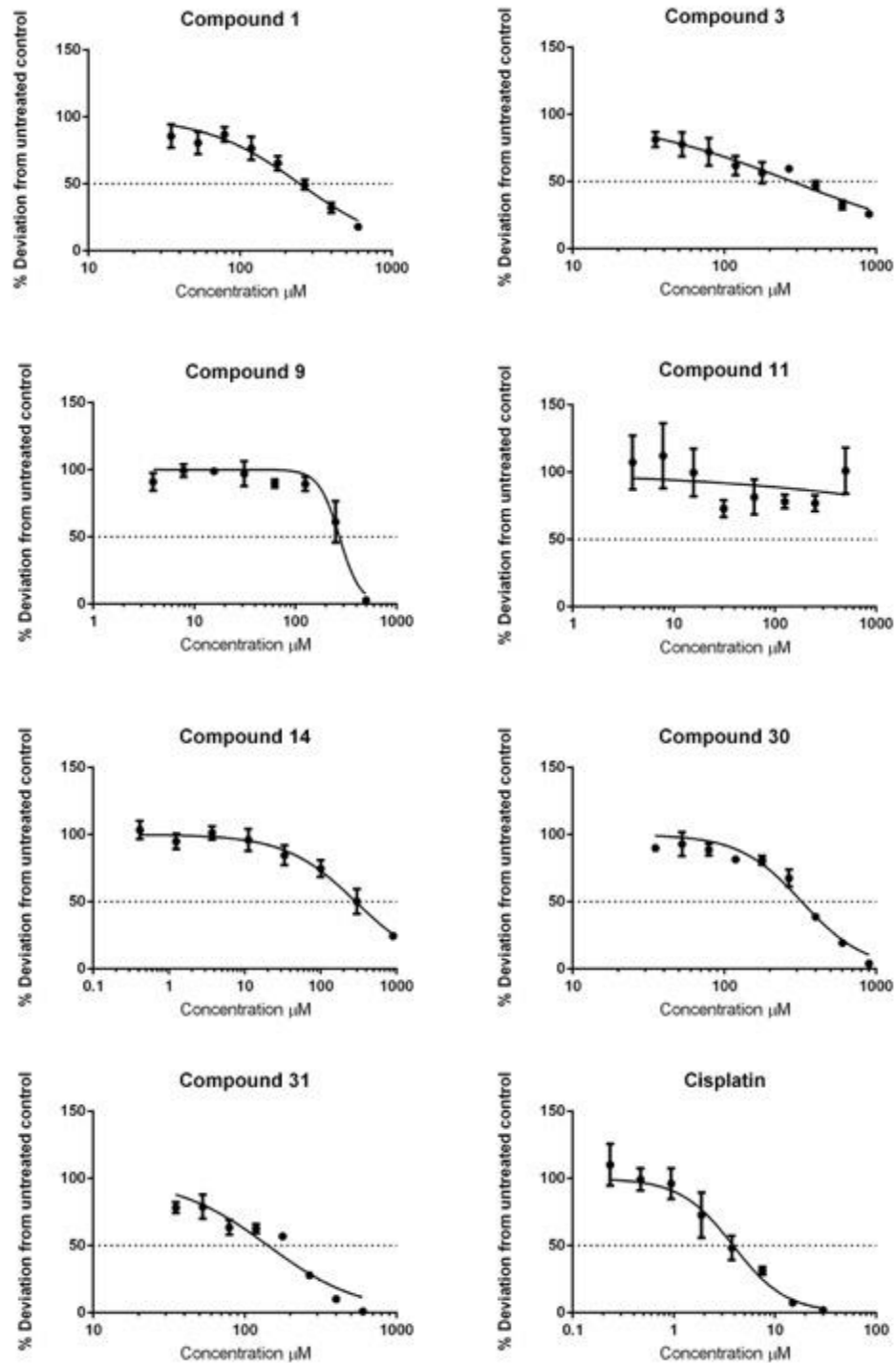


**Figure 3.6: Cell viability curves of U87MG cells treated with Compound 1, 3, 9, 11, 14, 30, 31 and Cisplatin for 96 hours.** Growth determined through SRB assay. Cells seeded at 6400 cpw and treated with compound after 48 hours. Plates left for further 96 hours, stopped and absorbance measured at 490nm. Data represents n=3 separate experiments.

### 3.4 Combination studies

#### 3.4.1 Chou-Talalay assay

The Chou-Talalay method was used to investigate whether these compounds and Cisplatin in combination showed any synergistic effects. A2780 cells were plated in 96 well plates at 800 cells per well and incubated for 48 hours, after which varying concentrations of the compound and Cisplatin were added to the cells and left for 96 hours. The absorbance was taken at 490nm and readings were analyzed in excel then input using CompuSyn software which gave a combination index value showing level of synergy. Synergy can be defined as “the effect of two or more agents working in combination that is greater than the expected additive effect of said agents”<sup>33</sup>. Numerically speaking, synergy is defined as a combination index  $<1$ , whilst additive is  $= 1$  and antagonism is  $>1$ .

When this method was used with Compound 1 (1-25), the results showed synergism of the drug combination. **Table 3.2** shows the combination index values obtained from CompuSyn for the combination of each drug concentration. The higher the level of synergy is colored in a darker purple, whereas the combination showing antagonistic or additive effects are colored in grey or white, respectively. Looking at **table 3.2**, it appears the levels of synergy are greater when lower concentrations of compound 1 are used.

**Figure 3.7** is a graph showing the effect of Cisplatin and Compound 1 alone, and also the effect of the two in combination. This graph demonstrates the synergistic effects of the combination, as the combination line is shifted to the left compared to the lines of just cisplatin and compound 1.

**Table 3.2:** Table showing combination index values and synergy levels of cisplatin and Compound 1 combination on A2780 cells. Data produced using Compusyn software (representative of n=4 individual experiments)

Combination Index values									
$\mu\text{M}$	C1 40	C1 20	C1 10	C1 5	C1 2.5	C1 1.25			Key to CI values
Cp 2.4	1.399	1.283	1.173	1.226	1.33	1.361	<0.1		Very strong synergism
Cp 1.2	1.169	1.103	1.023	1.024	0.95	1.113	0.1-0.3		Strong synergism
Cp 0.6	1.119	0.953	0.912	0.916	0.804	0.689	0.3-0.7		Synergism
Cp 0.3	1.022	0.974	0.868	0.659	0.778	0.672	0.7-0.85		Moderate synergism
Cp 0.15	0.948	0.976	0.72	0.679	0.648	0.531	0.85-0.95		Slight synergism
Cp 0.07	1.077	1.163	0.859	1.038	0.939	0.809	0.95-1.05		Additive
							>1.05		Antagonism

Combination assay comparing Cisplatin and Compound 1 on A2780 cells over 96 hours

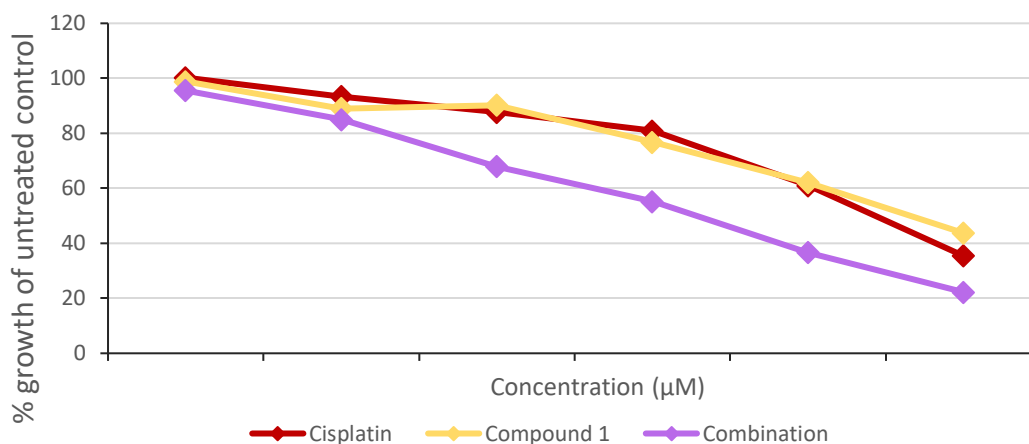


**Figure 3.7:** Graph showing effects of Cisplatin and Compound 1 both alone and in combination on A2780 cells. Cells treated for 96 hours, plated at 800 cells per well. (representative of n=4 individual experiments)

When compound 31 (2-35) was used, the analysis showed mainly antagonistic or additive effects with some low levels of synergy. The synergy shown also appeared to be at lower concentrations of compound 31, such as the result of the compound 1 combination study. In the graph in **figure 3.8**, the combination line is slightly shifted to the left, but not as noticeable a shift as seen with compound 1. This demonstrates that the synergistic effects are greater with compound 1 than they are with compound 31.

**Table 3.3:** Table showing combination index values and synergy levels of cisplatin and Compound 31 combination on A2780 cells. Data produced using Compusyn software. (representative of n=3 individual experiments)

Combination index values							Key to CI values
$\mu\text{M}$	C31 40	C31 20	C31 10	C31 5	C31 2.5	C31 1.25	
Cp 2.4	1.765	1.434	1.161	1.048	0.99	1.097	<0.1 Very strong synergism
Cp 1.2	1.55	1.29	1.106	0.991	1.136	1.057	0.1-0.3 Strong synergism
Cp 0.6	1.364	1.212	1.268	0.943	0.99	0.927	0.3-0.7 Synergism
Cp 0.3	1.195	1.295	1.032	0.923	0.898	0.97	0.7-0.85 Moderate synergism
Cp 0.15	1.239	0.889	0.879	0.907	0.843	1.093	0.85-0.95 Slight synergism
Cp 0.07	1.058	1.129	0.78	0.775	0.541	0.637	0.95-1.05 Additive
							>1.05 Antagonism

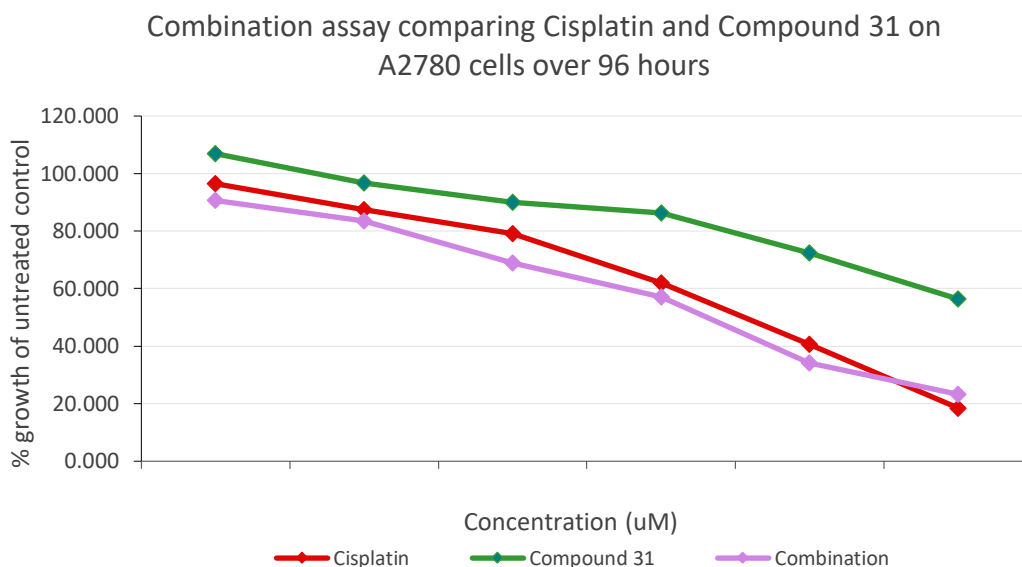


**Figure 3.8:** Graph showing effects of Cisplatin and Compound 31 both alone and in combination on A2780 cells. Cells treated for 96 hours, plated at 800 cells per well. (representative of n=3 individual experiments)

### 3.4.2 Drug combination assay

The Chou Talalay method was used to investigate the effects of combining Cisplatin with the SSA compounds. However, this method limits the minimum concentrations of Compound 1 which can be used as each compound must demonstrate a cytotoxic effect by itself at each concentration used. The results of the Chou-Talalay assay suggested that synergy was greater at low concentrations of compound 1 so in order to further explore the effects of this combination, a different assay was used in which A2780 cells were treated with the same concentration range of Cisplatin, but lower concentrations of Compound 1 were added. This allowed the concentration to be lower than their range used in the Chou-Talalay assay to less than the  $IC_1$  of Compound 1. For this assay the concentrations of Compound 1 used were the  $IC_{10}$  ( $8\mu M$ ),  $IC_5$  ( $4\mu M$ ),  $IC_{2.5}$  ( $2\mu M$ ),  $IC_1$  ( $0.8\mu M$ ) and the  $IC_{0.25}$  ( $0.2\mu M$ ).

These studies showed that lower concentrations of Compound 1 did not have as much of a synergistic effect as predicted from the results of the Chou-Talalay assay. This suggests that the synergistic effects shown previously are only significant down to a certain concentration below which there is an antagonistic effect. As shown in **figure 3.9**, when cisplatin was combined with the  $IC_{10}$ , the  $IC_5$  and the  $IC_{2.5}$  of compound 1, the curve was shifted to the left showing that these concentrations exert synergistic effects, however when the  $IC_1$  and the  $IC_{0.25}$  was added, the curve was shifted in the opposite direction, showing an antagonistic effect.

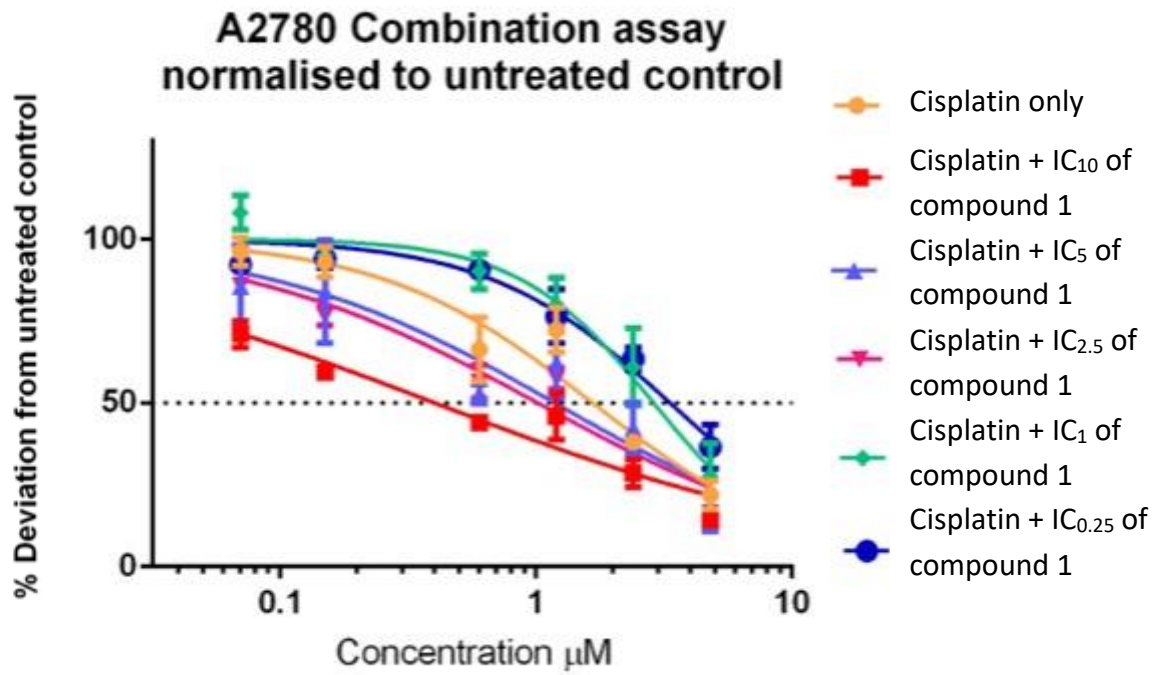


**Figure 3.9: Graph showing effects of Cisplatin alone and with different concentrations of Compound 1 on A2780 cells.** Cells treated for 96 hours, plated at 800 cells per well. (representative of 3 individual experiments)

### **3.5 Western blot analysis**

Western blotting was used to detect levels of selected proteins in the A2780 cell line when cells were treated to high and low concentrations of compound 1 and cisplatin both alone and in combination. Proteins investigated included those involved in the DNA damage response pathway, cell signalling proteins and also several cell cycle proteins. GAPDH was used as a loading control as it is constitutively expressed in all cell lines.

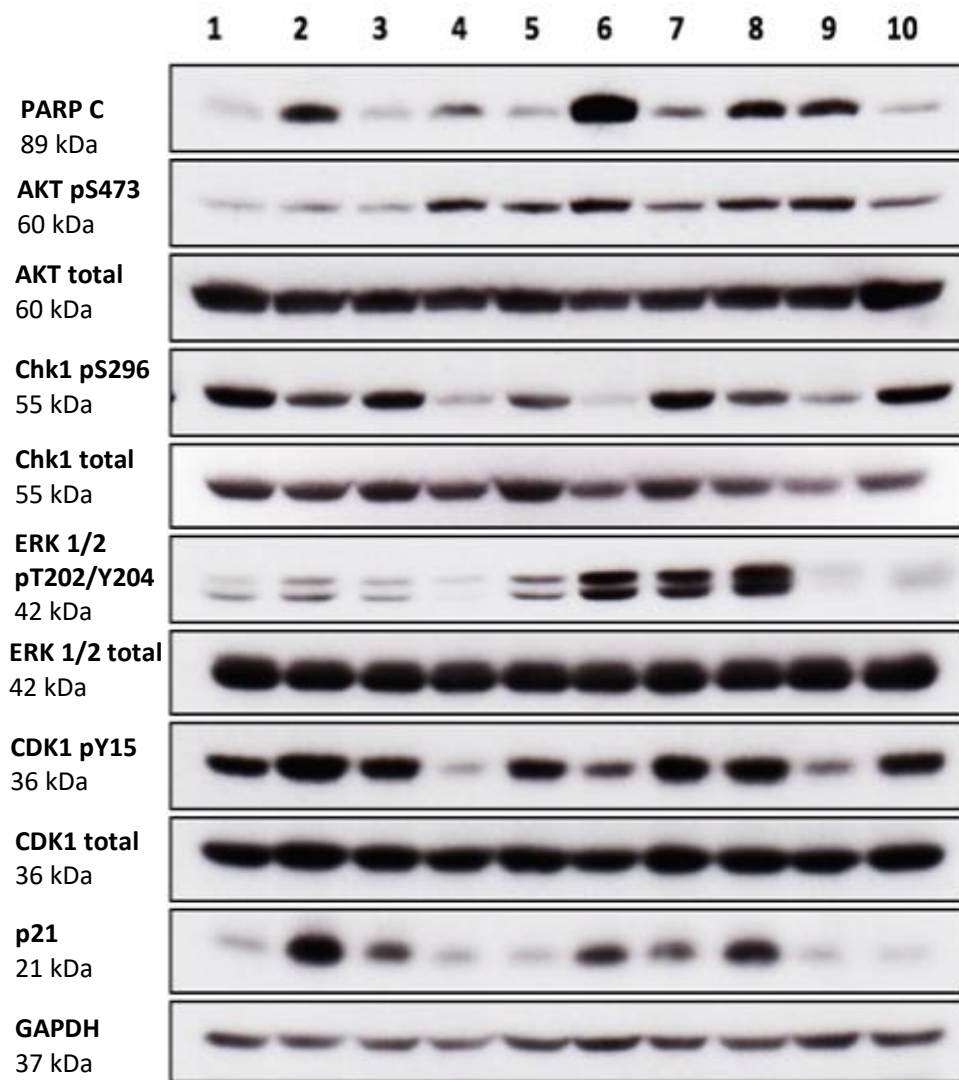
#### **The concentrations of Compound 1 and Cisplatin used are stated below**

**High Cisplatin:** 10 $\mu$ M (approximately 10x IC<sub>50</sub>)

**Low Cisplatin:** 1 $\mu$ M (approximately 1x IC<sub>50</sub>)

**High Compound 1:** 400 $\mu$ M (approximately 10x IC<sub>50</sub>)

**Low Compound 1:** 40 $\mu$ M (approximately 1x IC<sub>50</sub>)



1: Untreated control      6: High Cisplatin + High Compound 1  
 2: High Cisplatin      7: Low Cisplatin + Low Compound 1  
 3: Low Cisplatin      8: High Cisplatin + Low Compound 1  
 4: High Compound 1      9: Low Cisplatin + High Compound 1  
 5: Low Compound 1      10: Ethanol control

**Figure 3.10: Western blot of A2780 cells treated with high and low concentrations of Compound 1 and Cisplatin.** Cells treated with drug for 24 hours. Approximately 70  $\mu$ g of protein loaded. GAPDH used as loading control. Data representative of 3 individual experiments.

### 3.5.1 Cleaved PARP

One of the protein targets probed for was cleaved PARP, a marker of DNA damage and apoptosis. As seen in **figure 3.10**, expression of cleaved PARP was greater in cells treated with Cisplatin, whereas cells treated with Compound 1 showed similar levels of cleaved PARP as the untreated and ethanol controls. The cells which were treated with a combination of cisplatin and compound 1 showed greater expression of cleaved PARP compared to the cells treated solely with cisplatin. This suggests that the effect of cisplatin as a DNA damaging agent is enhanced by the presence of compound 1, supporting the theory that the two work together to produce synergistic effects.

### 3.5.2 Cell signalling targets

Proteins involved in major cell signalling pathways were also looked at, these include AKT phosphorylated at serine 473 (pS473) and total AKT from the PI3K/AKT pathway and also ERK 1/2 phosphorylated at threonine 202/tyrosine 204 and total ERK 1/2 which are involved in the MAPK pathway.

Cells treated with high compound 1 had a noticeable decrease in expression of phosphorylated ERK, and when treated with just cisplatin there was a slight increase in expression. However, when compound 1 and cisplatin were used in combination, the expression of phosphorylated ERK was greatly increased compared to either one alone. Expression of phosphorylated AKT appeared to increase in response to high and low levels of compound 1. The levels of phosphorylated AKT did not have much change in

cells treated with cisplatin alone, but when cells were treated with cisplatin and compound 1 there was a noticeable increase in expression.

### **3.5.3 Cell cycle proteins**

Several cell cycle proteins were also investigated, such as p21<sup>(Cip1/Waf1)</sup>, phosphorylated cyclin dependent kinase 1 (CDK1) and total CDK1 as well as phosphorylated checkpoint kinase 1 (Chk1) and total Chk1.

Expression of Chk1 phosphorylated at serine 296 appeared to decrease in cells treated with Compound 1, with the signal nearly completely knocked out in those treated with high concentration of the compound. Cells treated with low cisplatin showed similar levels of phosphorylated Chk1 as the untreated and ethanol controls, whereas those treated with high cisplatin showed slight decrease in expression.

CDK1 phosphorylated at tyrosine 15 showed similar levels to the basal expression in the untreated control when treated with both high and low cisplatin, with a slight increase in response to high cisplatin. When treated with high compound 1 alone and in combination, the signal of phosphorylated CDK1 was greatly decreased, whereas when treated with low compound 1, the signal was similar to that of the untreated control.

The p21<sup>(Cip1/Waf1)</sup> cyclin-dependent kinase inhibitor (CKI), was overexpressed in cells treated with high and low levels of Cisplatin, whereas when treated with just compound 1 there was no change in expression compared to the untreated and ethanol controls. The expression of p21 appeared to be greater in cells treated with just cisplatin as opposed to those treated with a combination of cisplatin and compound 1.

### 3.5.4 Western blot of Gamma H2AX

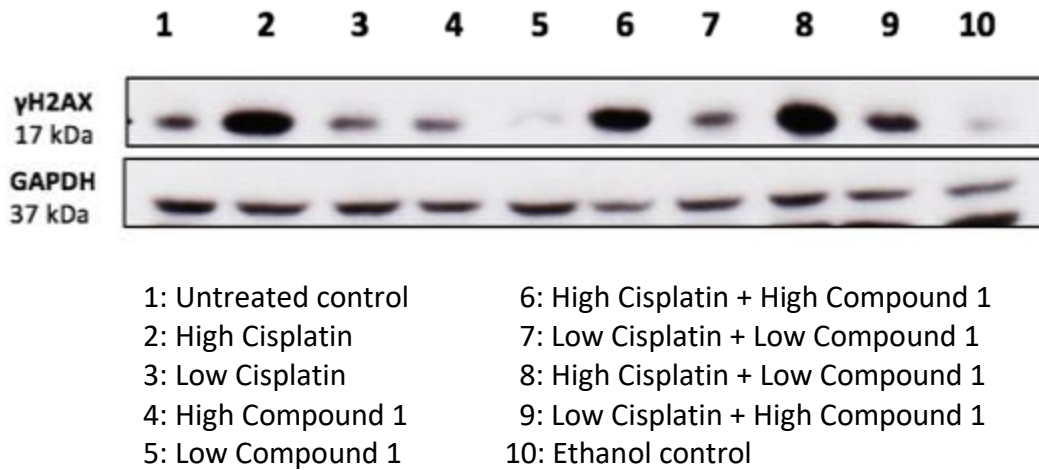


**Figure 3.11: Western blot of gamma H2AX in A2780 cells treated with high and low concentrations of Compound 1 and Cisplatin.** Cells treated with drug for 24 hours. Approximately 70  $\mu$ g of protein loaded. GAPDH used as loading control. Data representative of 3 individual experiments.

Gamma H2AX ( $\gamma$ H2AX) was probed for as it is a marker of DNA damage by double strand breaks (DSBs). As shown in **figure 3.11**, the expression of  $\gamma$ H2AX was greater in cells treated with high levels of cisplatin, which is expected as cisplatin is a known DNA damaging agent. The untreated and ethanol control showed very low levels of basal  $\gamma$ H2AX expression, and the cells treated with high and low levels of compound 1 alone showed nearly no expression of the protein. The combination of low cisplatin with high compound 1 (9) showed higher levels of  $\gamma$ H2AX expression compared to low cisplatin alone (3). The combination of high cisplatin with low compound 1 (8) also seemed to show a slight increase in expression when compared to high cisplatin alone (2).

### 3.6 Immunofluorescence

Immunofluorescence was used to visualize the interaction between the fluorescent compounds and cells. Compounds 30 and 31 have groups which allow them to fluoresce. A2780 cells were treated with Compound 31 and images were taken using a fluorescent microscope. Compound 31 could be clearly seen to bind to the membrane of the cells after immediate addition, and after incubation for an hour they could be seen to enter the cells and bind to some intercellular structures. When compound 31 was added, the cell membrane appeared to undergo blebbing which is indicated with the white arrows in **figure 3.12**.

Compound 30 was also able to bind the cell membrane on both cell lines as shown in **figure 3.13 (2)** and **figure 3.14 (2)** and could enter the cells, but did not bind the membrane as efficiently as compound 31.

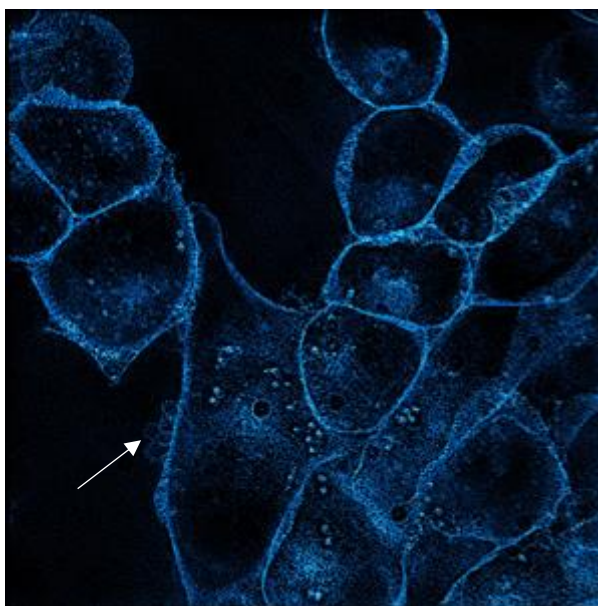


**Figure 3.12: Immunofluorescence of A2780 cells treated with Compound 31 (2-35) for 1 hour. DAPI filter image of A2780 cells, treated with 90uM Compound 31.**

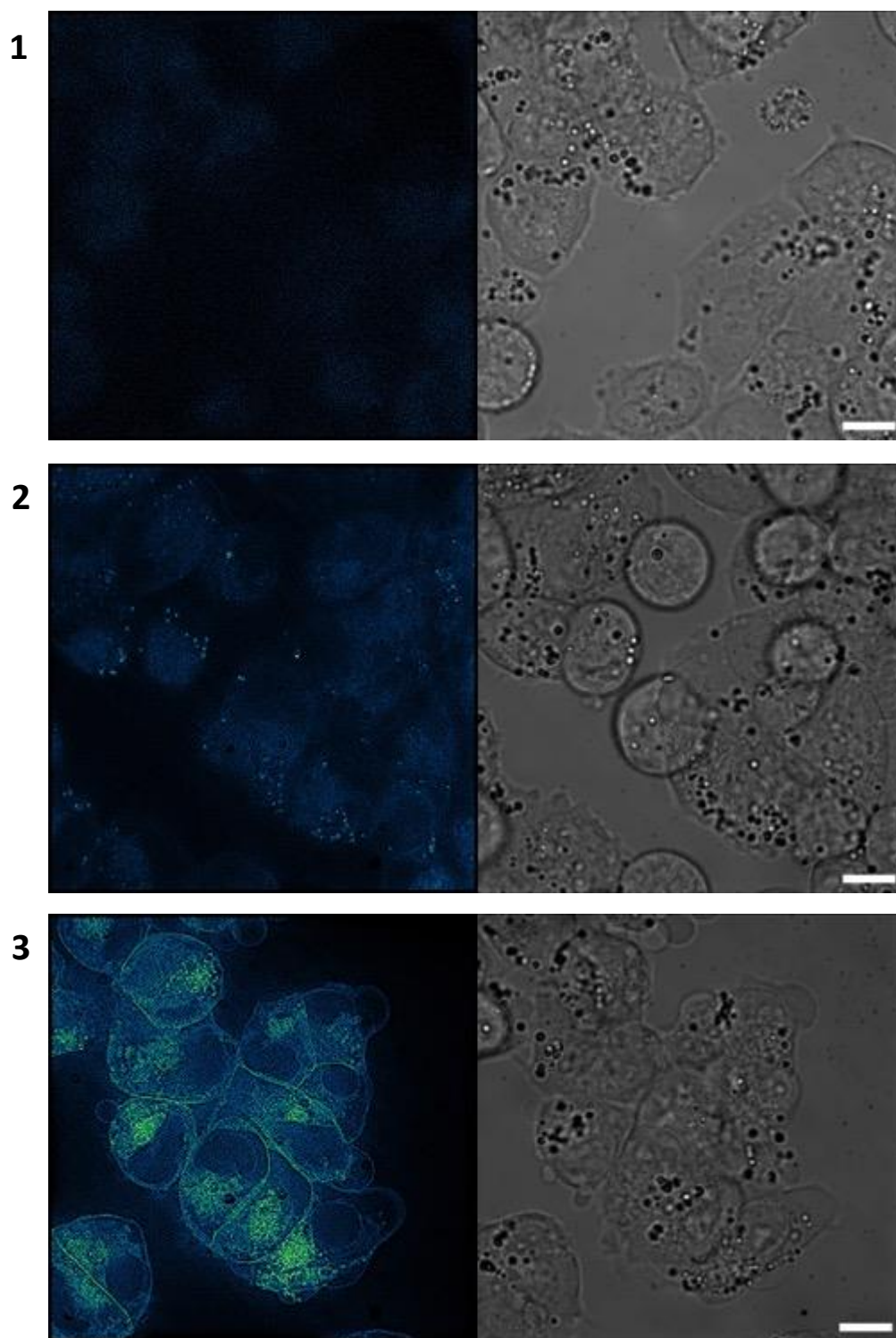


**Figure 3.13: Live cell fluorescence microscopy images of A2780 cells. 1: untreated A2780 cells, 2: A2780 cells after immediate addition of 180 $\mu$ M Compound 30, 3: A2780 cells after immediate addition of 90 $\mu$ M Compound 31. Left: DAPI filter fluorescent light. Right: Transmitted light**

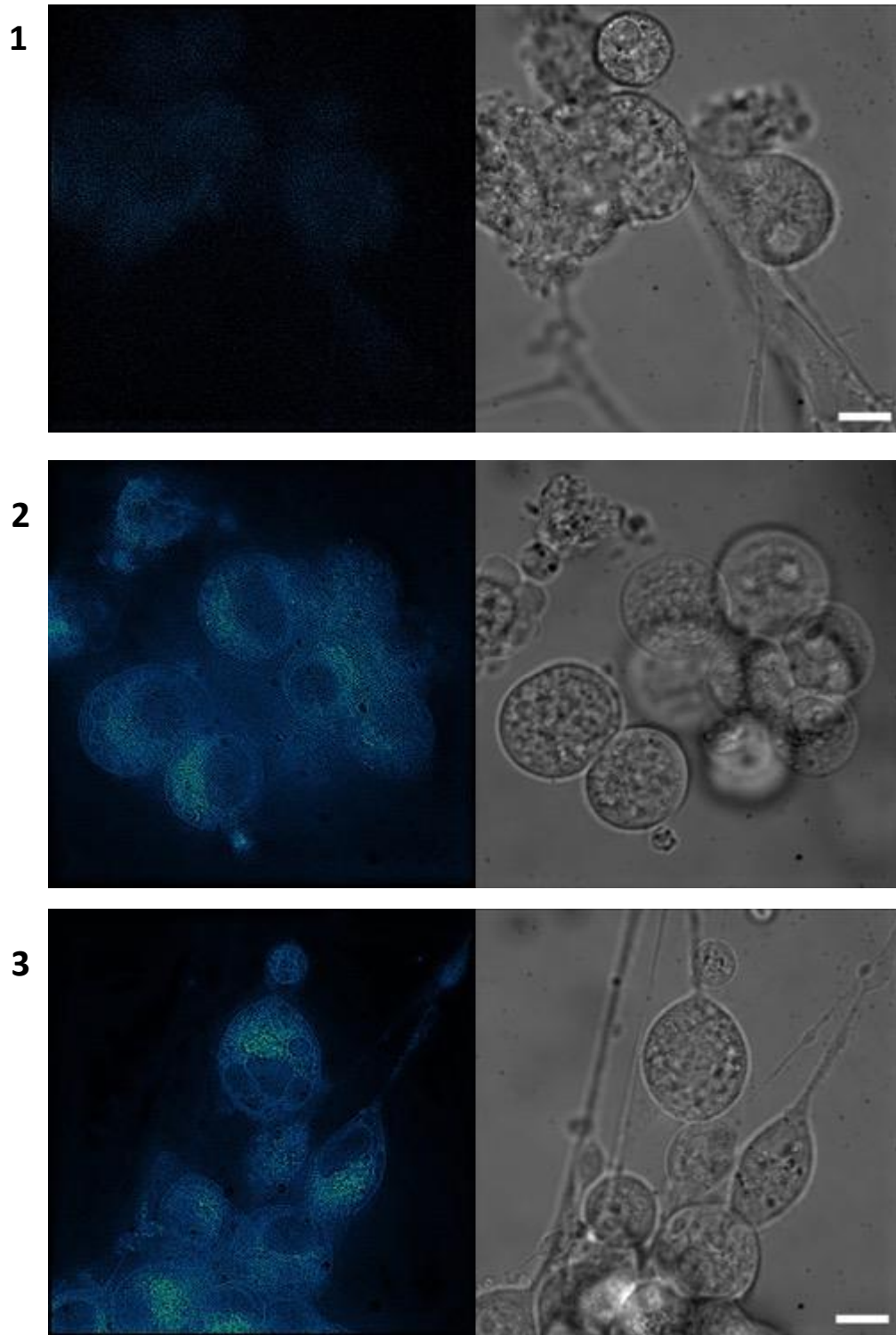


**Figure 3.14: Live cell fluorescence microscopy images of U87MG cells. 1:** untreated U87MG cells, **2:** U87MG cells after immediate addition of 900µM Compound 30, **3:** U87MG cells after immediate addition of 600µM Compound 31.

Left: DAPI filter fluorescent light. Right: Transmitted light

## **4. Discussion**

### **4.1 Introduction**

The aims of this project were to investigate the effect of novel antimicrobial compounds, known as supramolecular self-associating amphiphiles (SSAs), on cancer cells. These compounds showed toxicity against both cell lines, but were not particularly potent compared to existing chemotherapy agents. Further experimental techniques were used to explore the potential of these SSA compounds to enhance the efficacy of existing cancer drugs, such as cisplatin. Cisplatin is a widely used form of chemotherapy used to treat many cancers including ovarian cancer but it does have a number of harmful side effects, as is the issue with most forms of chemotherapy offered to patients currently. These compounds were also investigated as a potential biomarker of tumors. As some of these compounds are intrinsically fluorescent, they could be potentially used as a fluorescent marker for surgical procedures.

### **4.2 SRB analysis**

Results of the SRB assays measuring cell viability showed that nearly all of the selected SSA compounds are toxic to cancer cells. All of the compounds were able to kill cells of the A2780 cell line whereas all but compound 11 were toxic when screened against U87MG cells, although some were more potent than others. The levels of toxicity of these compounds showed the same trend across both cell lines.

Although these compounds themselves exhibit toxicity against cancer cells, they are not comparable to cancer drugs currently in clinical use. So their potential for

development as a form of cancer treatment by themselves is not feasible as there are already more efficient drugs available.

### **4.3 Chou Talalay**

The Chou Talalay method was used to investigate whether the compounds showed any synergism when used in combination. Synergy in drug combination is when the overall effect of two compounds is greater than the effect of each alone. When this data is analyzed using CompuSyn software, a combination index value is produced for drug combinations. Synergy is defined as a combination index value of  $<1$ , whilst additive is  $= 1$  and antagonism is  $>1$ . As the results show, the combination of compound 1 and Cisplatin showed synergistic effects at lower concentrations of compound 1. The effects were antagonistic when the concentration of Compound 1 was increased. This suggests that low concentrations of Compound 1 may have an effect that increases the efficacy of Cisplatin

When this technique was used with the combination of compound 31 and cisplatin it did not show the same trend. The effects were mainly antagonistic although there were some low levels of synergy, also exhibited by low concentrations of the compound. This suggests that the difference in the R group of compound 31 lessens its synergistic effects, indicating that compound 31 and 1 may have slightly different modes of action.

#### 4.4 Combination studies

The results of the Chou-Talalay assays showed that low concentrations of compound 1 tend to exert synergistic effects when combined with cisplatin. However, this assay limits the minimum concentrations that can be used. To further explore this hypothesis, a slightly different assay was conducted to assess the effects of compound 1 and cisplatin combination. This combination study allowed the synergistic effects to be further tested below the lower limits of the Chou-Talalay assay.

This assay looked at the effects of cisplatin on A2780 cells when combined with very low concentrations of compound 1. The Chou Talalay assay suggested that the lower the concentration of compound 1, the higher the synergistic effect. However, the results of this assay showed that there is in fact a limit to this effect, and at too low concentrations there is no synergy shown. This assay allowed the determination of the lower limits of compound 1 concentration which would allow synergy. The lowest concentrations used; the  $IC_{0.25}$  ( $0.2\mu M$ ) and  $IC_1$  ( $0.8\mu M$ ) of Compound 1 did not show synergistic effects. Comparing these results with the Chou-Talalay results, it appears the synergistic effects of compound 1 are the most prominent at a concentration between  $1.25\mu M$  and  $5\mu M$ .

The results of these combination studies may suggest some exciting clinical implications. Synergy is an area of interest in the development of cancer therapeutics as most chemotherapy drugs available have unpleasant and potentially harmful side effects. If multiple drugs are shown to exert synergy, this means that they may be

administered together at lower doses than they would be by themselves which consequently may reduce or possibly get rid of the unfavourable side effects whilst still having the intended outcome of tumor depletion.

#### **4.5 Western**

In order to gain more insight into the mechanism of these compounds, western blot analysis was used to detect levels of certain proteins in the cells. This experimental method can provide more information on the mode of action of the compounds and which area of the cell they are targeting.

##### **4.5.1 DNA damage**

Some of the protein targets looked at were involved in DNA damage, including gamma H2AX ( $\gamma$ H2AX) and cleaved Poly (ADP-ribose) polymerase 1 (PARP). These targets were chosen to see if the SSA compounds were targeting the nucleus in the cell and causing damage to the DNA.

The histone H2A variant, H2AX, is locally phosphorylated on serine 139 in response to DNA double strand breaks (DSBs) thus becoming  $\gamma$ H2AX<sup>31</sup>. H2AX phosphorylation occurs in the SQ motif located at the carboxy terminus of the protein, and this phosphorylation event can be carried out by a number of members of the phosphatidylinositol-3-OH-kinase like family of protein kinases (PIKKs)<sup>35</sup>, including the three major members; ATM, ATR and DNA-PKcs<sup>36,37</sup>. Gamma H2AX is widely used in research as a marker for DNA damage by DSBs<sup>38</sup>.

PARP1 is a 116 kDa, nuclear polymerase<sup>39</sup>. In response to extensive DNA damage by single strand breaks (SSBs), PARP1 is cleaved by caspase-3 between Asp214 and Gly215 to form two smaller protein fragments of 24 kDa (the PARP amino-terminal DNA binding domain) and 89 kDa (the carboxy-terminal catalytic domain)<sup>40</sup>. This cleavage event results in the inactivation of its DNA repair function. This allows the cells to undergo apoptosis instead as it would be more energy efficient than repairing the DNA. This means cleaved PARP can be used as a marker for apoptosis<sup>41</sup>.

As seen in **figure 3.10**, both  $\gamma$ H2AX and cleaved PARP showed increased expression in A2780 cells treated with just cisplatin, which is the expected result as cisplatin is a known DNA damaging agent. On the other hand, the cells treated with high concentrations of compound 1 alone showed an equal level of expression to the untreated control. This reveals that compound 1 does not cause damage to the DNA, and so suggests that compound 1 does not target the nucleus. Assuming that these compounds have a similar mechanism of action, these results can be supported by the immunofluorescence experiments, which demonstrated that compound 31 is able to bind to the plasma membrane and enter the cell to bind to intracellular structures but does not show any activity in the nucleus. Cells treated with a combination of cisplatin and compound 1 showed greater expression of cleaved PARP than those treated with cisplatin alone. This indicates that the action of compound 1 is resulting in increased efficacy of cisplatin as it signifies increased induction of the DDR pathway and resulting

apoptosis. This supports the theory of compound 1 having synergistic effects with cisplatin.

#### 4.5.2 Cell signalling targets

Other protein targets investigated were those involved in cellular signalling pathways, including the MAPK pathway and the PI3K/AKT pathway. AKT is a serine/threonine kinase and is a downstream target of PI3K which is activated through phosphorylation on the serine 473 residue at the carboxy terminus. Once activated, AKT signals through various downstream proteins including Bad, caspase-9<sup>42,43</sup> and forkhead transcription factors. AKT is normally upregulated in cancer cells to allow a tumor to survive as it can promote protein synthesis, cell survival and proliferation. AKT can influence the cell cycle as it can negatively regulate CDKs including p21 and p27<sup>44</sup>. The highly conserved PI3K/AKT pathway can be activated through membrane receptors such as EGFR and HER2. Looking at **figure 3.10**, it seems that phosphorylated AKT is upregulated in cells treated with compound 1 this may be a result of compound 1 targeting the membrane and causing the activation of PI3K which then in turn activates AKT. As the mechanism of these compounds is not fully understood, further experiments would be required to explore the meaning of these results.

ERK is part of the MAPK family of serine/threonine kinases which plays a role in a number of cellular processes, including differentiation, proliferation and death. ERK 1/2 is phosphorylated by MEK proteins on the activation loop residues at threonine 202 and tyrosine 204. Several studies have demonstrated a link between the activation

of ERK in response to cisplatin<sup>45,46,47</sup>, and it is thought activation of ERK mediates cell cycle arrest through phosphorylation of p53 to encourage DNA repair. The western blot in **figure 3.10**, shows a slight upregulation in ERK expression in cisplatin treated cells, but a noticeable increase in ERK expression in cells which had a combination of cisplatin and compound 1 compared to cisplatin alone. This result further supports the theory of synergy shown by compound 1 and cisplatin combination.

#### 4.5.3 Cell cycle proteins

The CKI p21<sup>(Cip1/Waf1)</sup> was also looked at, p21 is a tumor suppressor protein which when activated, is able to halt the cell cycle. The p53 tumor suppressor protein can be phosphorylated in response to cellular stress and this then has downstream effects to induce transcription of p21<sup>48</sup>. p21 can associate with and inhibit CDK complexes, stopping their kinase activity and arresting the cell cycle so it cannot progress through G1/S phase<sup>49</sup>. From the western blots in **figure 3.10**, it appears that p21 is upregulated in response to cisplatin treatment which is likely due to the DNA damage caused by cisplatin, which triggered the activation of p21 in order to halt the cell cycle so cells could not complete their division cycle with damaged DNA<sup>50</sup>. As compound 1 caused no change in the expression of p21, this supports the hypothesis that compound 1 does not target the nucleus and does not cause DNA damage.

Cyclin dependent kinase 1 (CDK1/Cdc2) also has a major role in cell cycle regulation and can trigger G2/M phase arrest<sup>51</sup>, which is a crucial checkpoint as this determines

whether the cell will proceed to mitosis or alternatively undergo apoptosis<sup>52</sup>. The expression of phosphorylated CDK1 displayed the same trend as Chk1 in the western blot studies. This is likely due to the same effect as these two proteins are involved in the same pathway. Checkpoint kinase 1 (Chk1) is an important cell cycle checkpoint which can be activated through phosphorylation by ATR at serine 345<sup>53</sup>. Chk1 phosphorylation can be triggered as a result of the DDR pathway activation<sup>54</sup>, and subsequently causes checkpoint activation and cell cycle arrest at the G1/S, intra S or G2/M phases to allow for DNA repair. This correlates with the western blot results as the Chk1 showed expression in cisplatin treated cells, but when treated with compound 1 the signal was not detectable which supports the hypothesis that compound 1 does not target the nucleus.

#### **4.6 Immunofluorescence**

The fluorescence microscopy experiments were conducted to assess how the compounds interact with the cell and to shed some light on their mechanism of action. Through these experiments as shown in **figure 3.13 and 3.14**, it was clear to see that both fluorescent compounds 30 (2-35) and 31 were able to bind the plasma membrane of both cell lines A2780 and U87MG. Compound 30 showed less efficient binding than compound 31 which supports the data produced from the compound toxicity assays. The IC<sub>50</sub> data produced through SRB analysis showed that compound 30 was less efficient at killing cancer cells on both A2780 and U87MG cell lines compared to compound 31. As seen in **table 3.1** Compound 30 had an IC<sub>50</sub> value of 59.53 ± 8.1 on

A2780 cells compared to  $29.61 \pm 9.7$  for compound 31, whilst compound 30 tested on U87MG cell line had an  $IC_{50}$  of  $367.3 \pm 48.5$  which is much higher than compound 31 which had an  $IC_{50}$  value of  $188.98 \pm 51.8$ .

Comparing these two fluorescent compounds, they have nearly identical molecular formulas however their structures vary slightly. Compound 31 has an added methyl group on the fluorophore element of the compound, and the arrangement of the fluorophore group is at a slightly different angle. The slight variation in structure is likely responsible for the difference in action of the two compounds. The positioning of the fluorophore group on compound 30 increases the distance between compounds, consequently the compounds are less likely to form intermolecular hydrogen bonds as the hydrogen bond accepting/ donating groups cannot get as close as compound 31, so they have lower affinity and therefore are less likely to form hydrogen bonds. This decreases the efficiency of the compounds as their proposed mechanism of action is based on their ability to form intermolecular hydrogen bonds and self-associate. This trend is also demonstrated in the antimicrobial studies conducted with these compounds. Compound 30 tested on MRSA and E. Coli showed far less toxic activity than compound 31<sup>25</sup>.

When A2780 cells were treated with compound 31, the immunofluorescence clearly showed the compound binding both the plasma membrane and intercellular structures, signs of membrane blebbing were also visible. Blebbing is a process which

occurs when cells are under stress conditions and is a marker of apoptosis. Blebbing is the formation of protrusions in the cell membrane, due to actomyosin contractions of the cortex allowing detachment of the membrane from the actin cortex after which cytosol leaves the main cell body to fill the bleb<sup>55</sup>.

A potential theory based on this evidence, is that the compounds target the plasma membrane and cause it to bleb resulting in disruption of the phospholipid bilayer thus allowing more efficient uptake of other molecules, such as cisplatin. This method would allow cisplatin to have a greater effect on cancer cells in combination with SSA compounds than when used by itself, which is supported by the synergy studies conducted.

#### **4.6.1 Tumor visualizing agent**

As shown through immunofluorescence, compound 31 is very efficient at binding membranes of cancer cells. There is potential for the fluorescent compounds to be developed as a visualization agent for tumors. Treating patients with these compounds could be useful as a targeted biomarker in surgical procedures. Using fluorescent compounds to target tumour cells is extremely beneficial in removing the bulk of the tumor. As surgery is normally the first line of treatment for most cancers, improving the efficacy of surgical removal could be a great opportunity for clinical use of these SSA compounds.

At present, there is a fluorescent tumor visualizing agent 5-ALA which is approved by the US FDA for use on high grade gliomas. This is informally known as the 'pink drink' as it is ingested orally by a patient prior to surgery. This compound can specifically bind to high grade glioma tumors and illuminates when exposed to fluorescent light.

Although this compound has been a useful aid in surgical procedures, it is limited to high grade tumors, which are more advanced and generally have poor patient prognosis. If a compound could be developed to be used on low grade tumors, this would be beneficial as a tumor could be removed in the earlier stages and when a patient's likelihood of survival is greater.

#### **4.7 Future works**

An important experiment to further carry out with these compounds would be to test them on healthy, non-cancerous 'normal' cell lines. If these are to be developed as a potential anti-cancer agent, they must be proven to be non-toxic to healthy cells.

##### **4.7.1 Further combination studies**

With more time, it would have been ideal to carry out combination studies on more of the compounds. Compound 1 was selected as it was one of the most effective compounds in terms of killing cancer cells. However, it would be interesting to look at some of the other effective compounds to see if they also have a synergistic effect, as perhaps some of the other range of compounds may exert greater synergy.

To further explore the synergistic effects exhibited by these compounds, it would be interesting to attempt the synthesis of cisplatin together with compound 1 and see whether this enhances delivery of cisplatin to cells. As these SSA compounds are hypothesized to form aggregates in solution, they may be able to be synthesized to form a mechanism of drug delivery straight to the cells by specifically binding to only cancer cell membranes. This method could also be tested with temozolomide and tested on brain tumor cells.

#### **4.7.2 Immunofluorescence**

Through immunofluorescence experiments, it is clear the fluorescent compound 31 is able to bind cancer cell membranes. There is a potential clinical implication of these SSA compounds as a tumor visualization agent as they are clearly able to bind both A2780 ovarian carcinoma cells and U87MG glioblastoma cells. 5-ALA, a fluorescent surgical marker is already approved for use on GBM. However, this compound is only beneficial for patients with high grade, advanced tumors. It would be interesting to test these SSA compounds on a low grade brain tumor cell line as if they are shown to have binding ability on low grade brain tumors, they could be developed as a potential new form of tumor biomarker.

#### **4.7.3 Protein analysis**

Given more time, further western blot analysis could be carried out to look at different signalling pathways in the cell to determine the exact mode of action of these compounds. Further western blot studies should also be done with other compounds,

in particular compound 31 to see whether they have the same effects as compound 1, which would reveal whether these compounds have a similar mode of action.

As western blotting only allows certain proteins to be looked at, it can be quite a limiting technique. Therefore, a potential experiment to try would be mRNA sequencing, which would provide an insight into the whole transcriptome of a cell. This would be an unbiased method of analyzing the levels of expression of all protein as opposed to just a selected few, and would aid in the understanding of the mechanism of these SSA compounds on mammalian cells<sup>56</sup>.

#### **4.8 Conclusion**

After conducting a number of experiments on the series of novel SSA compounds as outlined above, it is possible to conclude that whilst they did not show significant toxicity against cancer cells when used by themselves, they did exhibit synergistic effects when used in combination with SSA compound 1, which has potential clinical implications to improve the use of current chemotherapy agents, such as cisplatin, which cause harmful side effects. The fluorescent SSA compounds were shown to be very efficient at binding cancer cell membranes, which may indicate a potential to be developed as a fluorescent biomarker to aid in surgical procedure.

## References

- 1: WHO <https://www.who.int/topics/cancer/en/> (2019)
- 2: Cancer Research UK, <https://www.cancerresearchuk.org/health-professional/cancer-statistics/worldwide-cancer> (2019)
- 3: Goodsell, D.S. (2006) The molecular perspective: Cisplatin. *Stem Cells*. 24:514–515.
- 4: Weiss, R.B., Christian, M.C. (1993) New cisplatin analogues in development. A review. *Drugs*. 46, 360–377.
- 5: Dobbin, Z.C., Katre, A.A., Steg, A.D., Erickson, B.K., Shah, M.M., Alvarez, R.D., Conner, M.G., Schneider, D., Chen, D., Landen, C.N. (2014) Using heterogeneity of the patient-derived xenograft model to identify the chemoresistant population in ovarian cancer. *Oncotarget*. 5:8750–8764.
- 6: Gil, S., Carmona, A., Martinez-Criado, G., Leon, A., Prezado, Y., Sabes, M. (2015) Analysis of platinum and trace metals in treated glioma rat cells by x-ray fluorescence emission. *Biol Trace Elem Res*. 163:177–183.
- 7: Zuur, C.L., Simis, Y.J., Verkaik, R.S., Schornagel, J.H., Balm, A.J., Dreschler, W.A., Rasch, C.R. (2008) Hearing loss due to concurrent daily low-dose cisplatin chemoradiation for locally advanced head and neck cancer. *Radiother Oncol*. 89:38–43.
- 8: Smittenaar, C.R., Petersen, K.A., Stewart, K., Moitt, N. (2016) Cancer Incidence and Mortality Projections in the UK Until 2035. *Brit J Cancer*. 115; 1147–1155.
- 9: Cancer Research UK <https://www.cancerresearchuk.org/health-professional/cancer-statistics/statistics-by-cancer-type/brain-other-cns-and-intracranial-tumours/incidence#ref-6> (2018)
- 10: Jiménez, A. J., Domínguez-Pinos, M. D., Guerra, M.M., Fernández-Llebrez, P., & Pérez-Fígares, J. M. (2014). Structure and function of the ependymal barrier and diseases associated with ependyma disruption. *Tissue barriers*, 2, e28426. doi:10.4161/tisb.28426.
- 11: Simons, M., Nave, K. A. (2016). Oligodendrocytes: Myelination and Axonal Support. *Cold Spring Harbor perspectives in biology*, 8(1), a020479. doi:10.1101/cshperspect.a020479.
- 12: Cancer Research UK <https://www.cancerresearchuk.org/about-cancer/brain-tumours/survival> (2019)

- 13: Galicich, J.H., French, L.A., Melby, J.C. (1961) Use of dexamethasone in treatment of cerebral edema associated with brain tumors. *Lancet*. 81:46–53.
- 14: Hadjipanayis, C.G., Stummer, W. (2019) 5-ALA and FDA approval for glioma surgery. *J Neurooncol*. 141:479–86.
- 15: Stummer, W., Stocker, S., Novotny, A., Heimann, A., Sauer, O., Kempfski, O., Plesnila, N., Wietzorrek, J., Reulen, H.J. (1998) In vitro and in vivo porphyrin accumulation by C6 glioma cells after exposure to 5-aminolevulinic acid. *J Photochem Photobiol B*. 45:160–169.
- 16: Walker, M.D., Alexander, E., Hunt, W.E. et al. (1978) Evaluation of BCNU and/or radiotherapy in the treatment of anaplastic gliomas. *J Neuro- surg* 49, 333-343.
- 17: Walker, M.D., Strike, T.A., Shelino, G.E. (1979) An analysis of dose-effect relationship in the radiotherapy of malignant gliomas. *Int J Radiat Oncol Biol Phys* 5, 1725-1731.
- 18: Esteller, M., Garcia-Foncillas, J., Andion, E., Goodman, S.N., Hidalgo, O.F., Vanaclocha, V. et al. (2000) Inactivation of the DNA-repair gene MGMT and the clinical response of gliomas to alkylating agents. *N Engl J Med*; 343: 1350–4.
- 19: Kufe, D.W., Frei, E., Holland, J.F., et al. Colvin M. (2010) Alkylating agents and platinum antitumor compounds. *Holland-Frei Cancer Medicine*. 8th ed. Shelton, Connecticut: People's Medical Publishing House.
- 20: Stupp, R., Mason, W.P., van den Bent, M.J. (2005) Radiotherapy plus concomitant and adjuvant temozolomide for glioblastoma. *N Engl J Med*.; 352:987–996.
- 21: Weller, M., Stupp, R., Reifenberger, G., Brandes, A.A., van den Bent, M.J., Wick, W. et al. (2010) MGMT promoter methylation in malignant gliomas: ready for personalized medicine? *Nat Rev Neurol*; 6: 39–51.
- 22: White, L.J., Wells, N.J., Blackholly, L.R., Shepherd, H.J., Wilson, B., Bustone, G.P., Runacres, T.J., Hiscock, J.R. (2017) Towards quantifying the role of hydrogen bonding within amphiphile self-association and resultant aggregate formation. *Chem. Sci*. 8:11, pages 7620-7630.
- 23: Tyuleva, S.N., Allen, N., White, L.J., Pépés, A., Shepherd, H.J., Saines, P.J., Hiscock, J.R., (2018). A symbiotic supramolecular approach to the design of novel amphiphiles with antibacterial properties against MSRA. *Chemical communications (Cambridge, England)*, 55(1), 95–98.

- 24: Vander Heiden, M.G. et al. (2009) Understanding the Warburg Effect: The Metabolic Requirements of Cell Proliferation. *Science*, 324, 1029-1033.
- 25: Shevchenko, A., Simons, K. (2010) Lipidomics: Coming to grips with lipid diversity. *Nat. Rev. Mol. Cell Biol.* 11, 593–598.
- 26: Zalba, S., ten Hagen, T.L.M. (2017) Cell membrane modulation as adjuvant in cancer therapy. *Cancer Treat. Rev.* 52, 48–57.
- 27: Tan, L. T., Chan, K. G., Pusparajah, P., Lee, W. L., Chuah, L. H., Khan, T. M., ... Goh, B. H. (2017). Targeting Membrane Lipid a Potential Cancer Cure? *Frontiers in pharmacology*, 8, 12.
- 28: Jarmusch, A.K., Alfaro, C.M., Pirro, V., Hattab, E.M., Cohen-Gadol, A.A., and Cooks, R.G. (2016). Differential Lipid profiles of normal human brain matter and gliomas by positive and negative mode desorption electrospray ionization - Mass spectrometry imaging. *PLoS ONE* 11.
- 29: Bleeker, F.E., Lamba, S., Leenstra, S., et al. (2009). IDH1 mutations at residue p.R132 (IDH1(R132)) occur frequently in high-grade gliomas but not in other solid tumors. *Hum Mutat.* 30(1):7–11.
- 30: Kang, M.R., Kim, M.S., Oh, J.E., et al. (2009) Mutational analysis of IDH1 codon 132 in glioblastomas and other common cancers. *Int J Cancer.* 125(2):353–5.
- 31: Cohen, A.L., Holmen, S.L., & Colman, H. (2013). IDH1 and IDH2 mutations in gliomas. *Current neurology and neuroscience reports*, 13(5), 345.
- 32: Roth V. (2006) Doubling Time Computing, Available from: <http://www.doubling-time.com/compute.php>
- 33: Greco W.R., Faessel H., Levasseur L. (1996). The search for cytotoxic synergy between anticancer agents: a case of Dorothy and the ruby slippers? *J. Natl. Cancer Inst.* 88, 699–700.
- 34: Rogakou, E.P., Pilch, D.R., Orr, A.H., Ivanova, V.S., Bonner, W.M. (1998) DNA double-stranded breaks induce histone H2AX phosphorylation on serine 139. *J. Biol. Chem.* 273:5858–5868.
- 35: Paull, T.T., Rogakou, E.P., Yamazaki, V., Kirchgessner, C.U., Gellert, M., Bonner, W.M. (2000) A critical role for histone H2AX in recruitment of repair factors to nuclear foci after DNA damage. *Curr. Biol.* 10:886–895.

- 36: Burma, S., Chen, B.P., Murphy, M., Kurimasa, A., Chen, D.J. (2001) ATM phosphorylates histone H2AX in response to DNA double-strand breaks. *J. Biol. Chem.* 276:42462–42467.
- 37: Wang, H., Wang, M., Wang, H., Böcker, W., Iliakis, G. (2005) Complex H2AX phosphorylation patterns by multiple kinases including ATM and DNA-PK in human cells exposed to ionizing radiation and treated with kinase inhibitors. *J. Cell. Physiol.* 202:492–502.
- 38: Kinner, A., Wu, W., Staudt, C., Iliakis, G. (2008). Gamma-H2AX in recognition and signaling of DNA double-strand breaks in the context of chromatin. *Nucleic acids research*, 36(17), 5678–5694.
- 39: Satoh, M., Lindahl, T. (1992) Role of poly(ADP-ribose) formation in DNA repair. *Nature*, vol: 356 (6367) pp: 356-358.
- 40: Nicholson, D., Ali, A., Thornberry, N., Vaillancourt, J., Ding, C., Gallant, M., Gareau, Y., Griffin, P., Labelle, M., Lazebnik, Y., Munday, N., Raju, S., Smulson, M., Yamin, T., Yu, V., Miller, D. (1995) Identification and inhibition of the ICE/CED-3 protease necessary for mammalian apoptosis. *Nature*, vol: 376 (6535) pp: 37-43.
- 41: Oliver, F., de la Rubia, G., Rolli, V., Ruiz-Ruiz, M., de Murcia, G., Murcia, J. (1998) Importance of Poly(ADP-ribose) Polymerase and Its Cleavage in Apoptosis. *Journal of Biological Chemistry* vol: 273 (50) pp: 33533-33539.
- 42: Cardone, M.H., Roy, N., Stennicke, H.R., Salvesen, G.S., Franke, T.F., Stanbridge, E., Frisch, S., Reed, J.C. (1998) Regulation of cell death protease caspase-9 by phosphorylation. *Science*. 282: 1318-1321.
- 43: Datta, S.R., Dudek, H., Tao, X., Masters, S., Fu, H., Gotoh, Y., Greenberg, M.E. (1997)  
Akt phosphorylation of BAD couples survival signals to the cell-intrinsic death machinery. *Cell*. 91: 231-241.
- 44: Zhou, B.P., Liao, Y., Xia, W., Spohn, B., Lee, M.H., Hung, M.C. (2001) Cytoplasmic localization of p21Cip1/WAF1 by Akt-induced phosphorylation in *HER-2/neu*-overexpressing cells. *Nature Cell Biology* 3, 245–252.
- 45: Wang, X., Martindale, J.L., Holbrook, N.J. (2000) Requirement for ERK activation in cisplatin-induced apoptosis. *J Biol Chem.* 275(50):39435–43.
- 46: Qin, X., Liu, C., Zhou, Y., Wang, G. (2010) Cisplatin induces programmed death-1-ligand 1(PD-L1) over-expression in hepatoma H22 cells via Erk/MAPK signaling pathway. *Cell Mol Biol*; 56(Suppl):OL 1366–72.

- 47: Basu A., Tu, H. (2005) Activation of ERK during DNA damage-induced apoptosis involves protein kinase C $\delta$ . *Biochem Biophys Res Commun.*;334(4):1068–73.
- 48: Wang, Y., Prives, C. (1995) Increased and altered DNA binding of human p53 by S and G2/M but not G1 cyclin-dependent kinases. *Nature* 376, 88-91.
- 49: Pestell, R.G. et al. (1999) The cyclins and cyclin-dependent kinase inhibitors in hormonal regulation of proliferation and differentiation. *Endocrine Rev.* 20, 501-34
- 50: Chen, H., Landen, C. N., Li, Y., Alvarez, R. D., & Tollefsbol, T. O. (2013) Enhancement of Cisplatin-Mediated Apoptosis in Ovarian Cancer Cells through Potentiating G2/M Arrest and p21 Upregulation by Combinatorial Epigallocatechin Gallate and Sulforaphane. *Journal of oncology*, 2013, 872957.
- 51: Evan, G.I., Vouaden, K.H. (2001) Proliferation, cell cycle and apoptosis in cancer. *Nature*. 411:342–348.
- 52: Bartkova, J., Horejsi, Z., Koed, K., Krämer, A., Tort, F., Zieger, K. et al. (2005) DNA damage response as a candidate anti-cancer barrier in early human tumorigenesis. *Nature*. 434:864–870.
- 53: Liu, Q., Guntuku, S., Cui, X.S., Matsuoka, S., Cortez, D., Tamai, K., Luo, G., Carattini-Rivera, S., DeMayo, F., Bradley, A., Donehower, L.A., Elledge, S.J. (2000) Chk1 is an essential kinase that is regulated by Atr and required for the G(2)/M DNA damage checkpoint. *Genes Dev.* 14(12):1448-59.
- 54: Dai, Y., Grant, S. (2010) New insights into checkpoint kinase 1 in the DNA damage response signaling network. *Clin Cancer Res.* 16: 376-383.
- 55: Charras, G.T. (2008) A short history of blebbing. *J. Microsc.*, 231, pp. 466-478.
- 56: Wang, Z., Gerstein, M., & Snyder, M. (2009). RNA-Seq: a revolutionary tool for transcriptomics. *Nature reviews. Genetics*, 10(1), 57–63.